

Koopman-based feedback design with stability guarantees

Robin Strässer, Manuel Schaller, Karl Worthmann, Julian Berberich, Frank Allgöwer

Abstract—We present a method to design a state-feedback controller ensuring exponential stability for nonlinear systems using only measurement data. Our approach relies on Koopman operator theory and uses robust control to explicitly account for approximation errors due to finitely many data samples. To simplify practical usage across various applications, we provide a tutorial-style exposition of the feedback design and its stability guarantees for single-input systems. Moreover, we extend this controller design to multi-input systems and more flexible nonlinear state-feedback controllers using gain-scheduling techniques to increase the guaranteed region of attraction. As the proposed controller design is framed as a semidefinite program, it allows for an efficient solution. Finally, we validate the proposed feedback design procedure by means of numerical examples.

Index Terms—Data-driven control, Koopman, nonlinear systems, robust control, stability, region of attraction

I. INTRODUCTION

CONTROL theory has recently encountered a shift towards data-driven methods by the increasing availability of measurement data. This trend is particularly prominent in the context of nonlinear systems, where classical approaches, such as system identification and first-principles modeling, prove time-consuming, require expert knowledge, and often lead to non-convex optimization problems [1]. Data-driven methods may circumvent these challenges by exploiting available data to construct a suitable representation of the underlying complex system that allows for a convex controller design.

While data-driven feedback design for linear systems with guarantees for the closed-loop system has been extensively investigated in the literature [2]–[5], obtaining rigorous guarantees for general nonlinear systems remains an open challenge, see also, e.g., [1], [6]–[8] and the references therein. Available stability guarantees for particular classes of nonlinear systems include, e.g., Hammerstein and Wiener systems [9], bilinear systems [10], polynomial systems [11], [12], and rational dynamics [13], where the resulting controller designs are based on semidefinite programs (SDP). For more general classes of nonlinear systems, an SDP-based controller design can

be achieved through approaches such as polynomial approximation [14], [15], Kernel regression [16], [17], or linear parameter-varying (LPV) embeddings [18], [19]. A comprehensive overview of data-driven control methods for nonlinear systems is provided in [1].

B.O. Koopman introduced a different perspective in his seminal paper of 1931 [20], offering an exact description of autonomous nonlinear dynamics through a linear, yet infinite-dimensional system. This approach views the system through the lens of observables evolving linearly over time, bridging the gap between nonlinear and linear control methods. Over the past two decades, the Koopman operator has gained widespread popularity [21]–[25]. For control-affine systems, the Koopman framework yields an infinite-dimensional bilinear operator, and a finite-dimensional matrix approximation is typically used for computational tractability. Common approximation techniques include extended dynamic mode decomposition (EDMD) [26]–[28] and machine learning methods [29], [30] (and the references therein). A probabilistic analysis of the resulting approximation error is given in [31]–[33] and was recently extended to kernel EDMD [34]. Although the majority of the existing approaches predominantly assume linear lifted dynamics or neglect the deviation between the infinite-dimensional lifted system and its finite-dimensional approximation [35]–[37], Koopman-based control has demonstrated success in a wide range of applications, cf. [38]–[40] and [24, Chapter III]. However, closed-loop guarantees can only be deduced by incorporating the approximation error into the controller design and its analysis. The work in [41] introduces a robust linear controller design for an error-perturbed bilinear lifted system in discrete time based on a linear fractional representation (LFR). Under the assumption of a given finite-gain bound on the approximation error resulting from a finite dictionary and a finite data set, this approach provides closed-loop guarantees for the underlying nonlinear system. However, the practical application is challenging, since the work does not provide a procedure on how to ensure the required finite-gain bound.

In this work, we introduce a robust controller design that rigorously ensures end-to-end stability for nonlinear systems using measurement data only. Based on previous work on the approximation error [32], [42], we establish a novel error bound for the Koopman generator, which is proportional to the state and control in dependence on the amount of data. This allows us to extend the controller design from our previous works [41], [43] to continuous time and solve the key technical challenge of stabilizing the original nonlinear system rather than some lifted bilinear one. Notably, this is possible without

F. Allgöwer is thankful that this work was funded by the Deutsche Forschungsgemeinschaft (DFG, German Research Foundation) under Germany’s Excellence Strategy – EXC 2075 – 390740016 and within grant AL 316/15-1 – 468094890. K. Worthmann gratefully acknowledges funding by the German Research Foundation (DFG; project number 507037103). R. Strässer thanks the Graduate Academy of the SC SimTech for its support.

R. Strässer, J. Berberich, and F. Allgöwer are with the Institute for Systems Theory and Automatic Control, University of Stuttgart, 70550 Stuttgart, Germany (email: {robin.straesser, julian.berberich, frank.allgower}@ist.uni-stuttgart.de)

M. Schaller and K. Worthmann are with the Institute for Mathematics, Technische Universität Ilmenau, 99693 Ilmenau, Germany (e-mail: {manuel.schaller, karl.worthmann}@tu-ilmenau.de).

having to switch between different coordinates but directly in terms of the *true* system state. Our results rely on an SDP in terms of linear matrix inequalities (LMI) which are efficiently solvable by standard software. The presented controller design establishes a connection between a probabilistic tolerance concerning closed-loop guarantees for the nonlinear system and the necessary amount of data needed to satisfy a predetermined bound on the approximation error of the lifted system. To enhance accessibility and implementation in a variety of applications, we provide a tutorial-style exposition of the proposed feedback design and its provable guarantees for a simplified setting with single-input systems. Moreover, we generalize the controller design to more flexible nonlinear state-feedback controllers, reducing conservatism and resulting in guarantees within a larger region of attraction (RoA). We evaluate the presented controller by means of various numerical examples, e.g., by illustrating the RoA in the original state space. The recent work [44] is related to our approach since it proposes a robust approach in discrete time using the Koopman operator and an LPV formulation, but the derived stability guarantees hold only if the LPV system is already open-loop stable.

This work is structured as follows. After providing the preliminaries for our approach in Section II, we derive a data-driven controller design for nonlinear systems using convex optimization. Section III provides the derivation of the proposed state-feedback controller design for single-input systems alongside a proof of closed-loop stability. We consider multi-input systems and a more general controller parametrization in Section IV. The geometry of the guaranteed RoA induced by the nonlinear lifting and the controller design is discussed in Section V. Finally, we apply the developed controller design to numerical examples in Section VI, before Section VII concludes the paper.

Notation: We write I_p for the $p \times p$ identity matrix and $0_{p \times q}$ for the $p \times q$ zero matrix, where we omit the index if the dimension is clear from the context. If A is symmetric, then we write $A \succ 0$ or $A \succeq 0$ if A is positive definite or positive semidefinite, respectively. Negative (semi)definiteness is defined analogously. Matrix blocks which can be inferred from symmetry are denoted by \star and we abbreviate $B^\top AB$ by writing $[\star]^\top AB$. We denote the Kronecker product by \otimes . We write $[n : m]$ for the interval of integers $[n, m] \cap \mathbb{Z}$ and use the short-hand notation $[m] := [1 : m]$. A function $f : \mathbb{R}^p \rightarrow \mathbb{R}^q$ belongs to the differentiability class $\mathcal{C}^k(\mathbb{F}, \mathbb{H})$ if the function is k times continuously differentiable on the domain $\mathbb{F} \subseteq \mathbb{R}^p$ mapping to $\mathbb{H} \subseteq \mathbb{R}^q$. Finally, we define the function class \mathcal{K} containing all functions $\alpha : [0, \infty) \rightarrow [0, \infty)$ which are continuous, strictly increasing, and satisfy $\alpha(0) = 0$.

II. PRELIMINARIES

In this section, we first introduce the problem setting (Section II-A) and then derive a data-driven representation of nonlinear systems using the Koopman operator (Section II-B).

A. Problem setting

In this paper, we consider *unknown* nonlinear control-affine systems of the form

$$\dot{x}(t) = f(x(t)) + \sum_{i=1}^m g_i(x(t))u_i(t), \quad (1)$$

where $x(t) \in \mathbb{R}^n$ denotes the state at time $t \geq 0$ and the control function $u \in L_{\text{loc}}^\infty([0, \infty), \mathbb{R}^m)$ serves as an input. The map $f : \mathbb{R}^n \rightarrow \mathbb{R}^n$ is called drift, while $g_i : \mathbb{R}^n \rightarrow \mathbb{R}^n$, $i \in [m]$ are called input maps. For initial condition $x(0) = \hat{x} \in \mathbb{R}^n$ and control function u , we denote the solution of (1) at time $t \geq 0$ by $x(t; \hat{x}, u)$ tacitly assuming its existence. We assume that $f(0) = 0$ holds, i.e., that the origin is a controlled equilibrium for $u = 0$.

The functions f and g_i , $i \in [m]$, are unknown and only data samples $f(x_j) + \sum_{i=1}^m g_i(x_j)u_i$ for suitably chosen input signals u_i and sampling points $x_j \in \mathbb{X} \subset \mathbb{R}^n$, $j \in [d]$ with $d \in \mathbb{N}$, are available. Here, \mathbb{X} is assumed to be compact and convex. Further, we will consider measurable controls with values in a compact set $\mathbb{U} \subset \mathbb{R}^m$ with $0 \in \text{int}(\mathbb{U})$. Our goal is the systematic design of a static state-feedback control law $\mu : \mathbb{R}^n \rightarrow \mathbb{R}^m$ such that the origin is exponentially stable w.r.t. the closed loop

$$\dot{x}(t) = f(x(t)) + \sum_{i=1}^m g_i(x(t))\mu_i(x(t)). \quad (2)$$

In particular, we want to guarantee exponential stability in a later defined RoA in terms of a Lyapunov-function sublevel set.

To construct a data-driven controller relying solely on the above mentioned samples of the system, we represent the nonlinear system (1) using the Koopman operator framework.

B. Data-driven system representation using the Koopman operator

In the following, we first introduce the considered Koopman operator framework and its finite-dimensional approximation using data samples. Then, we discuss suitable error bounds on the resulting approximation error.

1) *Koopman operator and its approximation:* The Koopman operator \mathcal{K}_t^u corresponding to the system dynamics (1) with constant control input $u \in \mathbb{R}^m$ is defined as

$$(\mathcal{K}_t^u \varphi)(\hat{x}) = \varphi(x(t; \hat{x}, u)) \quad (3)$$

for all $t \geq 0$, $\hat{x} \in \mathbb{X}$, $\varphi \in L^2(\mathbb{X}, \mathbb{R})$, where the real-valued functions φ are called *observables* [20]. Here, we tacitly assumed invariance of \mathbb{X} under the flow such that the observable functions are defined on $x(t; \hat{x}, u)$ for all $\hat{x} \in \mathbb{X}$. This assumption can be relaxed by considering initial values contained in a tightened version of \mathbb{X} , see, e.g., [45] for details. For this setting, $(\mathcal{K}_t^u)_{t \geq 0}$ is a strongly-continuous semigroup of bounded linear operators, i.e., we can define its infinitesimal generator \mathcal{L}^u via

$$\mathcal{L}^u \varphi := \lim_{t \searrow 0} \frac{\mathcal{K}_t^u \varphi - \varphi}{t} \quad \forall \varphi \in D(\mathcal{L}^u), \quad (4)$$

where the domain $D(\mathcal{L}^u)$ consists of all L^2 -functions for which the above limit exists. By definition of this generator, the propagated observable satisfies $\dot{\varphi}(x) = \mathcal{L}^u \varphi(x)$.

A crucial structural property of this generator is that it preserves control affinity [46]–[48], i.e., for $u \in \mathbb{R}^m$ we obtain

$$\mathcal{L}^u = \mathcal{L}^0 + \sum_{i=1}^m u_i (\mathcal{L}^{e_i} - \mathcal{L}^0), \quad (5)$$

where \mathcal{L}^0 and \mathcal{L}^{e_i} , $i \in [m]$, are the generators of the Koopman semigroups corresponding to the constant control functions $u \equiv 0$ and $u \equiv e_i$ with the unit vector e_i , $i \in [m]$, respectively.

A data-driven approximation of the Koopman operator or its generator can now be constructed via EDMD [26] or generator EDMD [49]. Therein, one learns a finite-dimensional version of the operators, so-called compressions, restricted onto the span of a finite number of observable functions by means of a finite number of samples. In these techniques, the approximation error usually consists of two sources: A deterministic projection error due to finitely many observable functions and a probabilistic estimation error due to finitely many data points, cf. [27] for the infinite-data limit and [32], [33], [50] for finite-data error bounds. An alternative route avoiding the a-priori choice of a dictionary is given by kernel EDMD, cf. [51], [52], see [34] for error bounds.

We define the dictionary $\mathbb{V} := \text{span}\{\phi_k\}_{k=0}^N$ representing the $(N+1)$ -dimensional subspace spanned by the chosen observables $\phi_k : \mathbb{R}^n \rightarrow \mathbb{R}$, $k \in [0 : N]$. We include a constant function and the full state in the observables, i.e., we define $\Phi : \mathbb{R}^n \rightarrow \mathbb{R}^{N+1}$ by $\phi_0(x) \equiv 1$ and $\phi_k(x) = x_k$ for $k \in [n]$ resulting in

$$\Phi(x) = [1 \quad x^\top \quad \phi_{n+1}(x) \quad \cdots \quad \phi_N(x)]^\top, \quad (6)$$

where $\phi_k \in \mathcal{C}^2(\mathbb{R}^n, \mathbb{R})$ satisfy $\phi_k(0) = 0$, $k \in [n+1 : N]$. Note that the constant observable $\phi_0 \equiv 1$ is included to account for state-independent input maps $g_i(x) = b_i$, $b_i \in \mathbb{R}^n$, $i \in [m]$.

Remark 1. *The consideration of dictionaries not containing the coordinate maps is an important issue if full state measurements are not available. In this case, when performing Koopman-based prediction and control, one has to resort to reprojecton techniques [45] to obtain a lifted state which is consistent with the structure of the dictionary, i.e., lies on the image of $\Phi(\mathbb{X}) := \{\Phi(x) \mid x \in \mathbb{X}\}$, and in view of numerical robustness.*

As the lifting Φ defined in (6) explicitly contains the full state x and satisfies $\phi_k(0) = 0$ for all $k \in [N]$, we get the lower bound

$$\|\Phi(x) - \Phi(0)\|^2 = \|x\|^2 + \sum_{k=n+1}^N \|\phi_k(x)\|^2 \geq \|x\|^2. \quad (7)$$

Further, a corresponding upper bound can be deduced via local Lipschitz continuity of the lifting function $\Phi(x)$, which is a direct consequence of $\Phi \in \mathcal{C}^1(\mathbb{R}^n, \mathbb{R}^N)$. In particular, there exists an $L_\Phi > 0$ such that

$$\|\Phi(x) - \Phi(0)\| \leq L_\Phi \|x\| \quad (8)$$

holds for all $x \in \mathbb{X}$.

Throughout the paper, we assume that the dictionary \mathbb{V} is invariant w.r.t. the dynamics in the following sense.

Assumption 2 (Invariance of \mathbb{V}). *For any $\phi \in \mathbb{V}$, the relation $\phi(x(t; \hat{x}, u)) \in \mathbb{V}$ holds for all $u(t) \equiv \hat{u} \in \mathbb{U}$, $\hat{x} \in \mathbb{X}$, and $t \geq 0$.*

Assumption 2 is commonly assumed when representing controlled systems via the Koopman operator. Sufficient conditions for (approximately) satisfying this assumption are provided, e.g., by [35], [53], [54]. If the dictionary \mathbb{V} does not fulfill the assumption, it is also possible to derive error bounds for the projection error [33], [34]. We note that [55] proposes to consider also a nonlinear dependence of the lifted dynamics on the input signal, whereas we only require state-dependent observables for our proposed controller. Further, [56] introduces a notion of proximal invariance using Jordan principal angles, which provides a promising route for formulating approximate invariance in future work.

We denote the L^2 -orthogonal projection onto the dictionary \mathbb{V} by $P_\mathbb{V}$. Then, Assumption 2 can be formulated compactly as

$$P_\mathbb{V} \mathcal{L}^u|_\mathbb{V} = \mathcal{L}^u|_\mathbb{V}, \quad (9)$$

i.e., the projection of $\mathcal{L}^u|_\mathbb{V}$ (the Koopman generator restricted to \mathbb{V}) onto \mathbb{V} is equal to $\mathcal{L}^u|_\mathbb{V}$. As a consequence, we obtain the Koopman operator for $u \in \mathbb{U}$ via $\mathcal{K}_t^u|_\mathbb{V} = e^{t\mathcal{L}^u|_\mathbb{V}}$.

We assume that the nonlinear dynamics (1) are unknown and we have state-derivative data $\{x_j^{\bar{u}}, \dot{x}_j^{\bar{u}}\}_{j=1}^{d^{\bar{u}}}$ for the constant control inputs $u(t) \equiv \bar{u}$, where $\bar{u} \in \{0, e_1, \dots, e_m\}$ and $d^{\bar{u}}$ denotes the number of data points for the control vector \bar{u} . Since the lifting functions are known, this allows constructing data samples $\{\phi_k(x_j^{\bar{u}}), \langle \nabla \phi_k(x_j^{\bar{u}}), f(x_j^{\bar{u}}) \rangle\}$ (or equivalently, $\{\Phi(x_j^{\bar{u}}), \dot{\Phi}(x_j^{\bar{u}})\}$), $k \in [0 : N]$ and $j \in [d^{\bar{u}}]$.

Throughout this paper, we assume that derivative measurements are available, which is a standard requirement in continuous-time data-driven control. It is also possible to derive analogous results for discrete-time systems without resorting to derivative measurements, compare [41], [42] for the required basics on Koopman-based estimation and control in discrete time.

We emphasize that we require sufficiently many snapshots for each of the $m+1$ open-loop dynamics corresponding to a constant control $\bar{u} \in \{0, e_1, \dots, e_m\}$. For the data generation, the control inputs e_i , $i \in [m]$, may be chosen as any basis of \mathbb{R}^m , e.g., in case of $0 \in \text{int } \mathbb{U}$, as scaled unit vectors to ensure their feasibility, i.e., $e_i \in \mathbb{U}$ for $i \in [m]$.

We briefly recall the consequences of the structure of the Koopman generator and the chosen dictionary and show how to design a suitable data-driven surrogate model as proposed in [42, Sec. 3.2]. The Koopman generator \mathcal{L}^u corresponding to the chosen dictionary defined in (6) has a particular structure due to the presence of the constant observable $\phi_0(x) \equiv 1$ satisfying

$$\frac{d}{dt} \phi_0(x(t; \cdot, u)) = \langle \phi_0(x(t; \cdot, u)), f(x(t; \cdot, u), u(t)) \rangle \equiv 0.$$

As $\frac{d}{dt} \phi_0(x(t; \cdot, u))$ corresponds to the first row of \mathcal{L}^u , we may infer that the first row of \mathcal{L}^u can only have zero entries for

all $u \in \mathbb{U}$. Hence, one may deduce that \mathcal{L}^0 and \mathcal{L}^{e_i} , $i \in [m]$, contain only zeros in their first row. Moreover, due to the assumption that the drift term of the dynamics (1) vanishes at the origin, i.e., $f(0) = 0$, we compute

$$(\mathcal{L}^0 \Phi)(0) = \nabla \Phi(0)^\top f(0) = 0, \quad (10)$$

i.e., in \mathcal{L}^0 there are no contributions from the constant observable $\phi_0(x) \equiv 1$. Hence, the first column of \mathcal{L}^0 must be zero. Thus, the generators are of the form

$$\mathcal{L}^0 = \begin{bmatrix} 0 & 0_{1 \times N} \\ 0_{N \times 1} & \mathcal{L}_{22}^0 \end{bmatrix}, \quad \mathcal{L}^{e_i} = \begin{bmatrix} 0 & 0_{1 \times N} \\ \mathcal{L}_{21}^{e_i} & \mathcal{L}_{22}^{e_i} \end{bmatrix}, \quad (11)$$

with $\mathcal{L}_{22}^0 \in \mathbb{R}^{N \times N}$ and $\mathcal{L}_{21}^{e_i} \in \mathbb{R}^{N \times 1}$, $\mathcal{L}_{22}^{e_i} \in \mathbb{R}^{N \times N}$, $i \in [m]$, respectively.

In the following, we show how to enforce this structure of the Koopman generator also for its data-driven surrogate model. Here, we use EDMD to obtain a data-based approximation \mathcal{L}_d^u of the true Koopman generator \mathcal{L}^u . Based on $d^{\bar{u}}$ data points for $\bar{u} \in \{0, e_1, \dots, e_m\}$ and the dictionary \mathbb{V} , we define the $((N+1) \times d^{\bar{u}})$ -matrices X^{e_i} for $i \in [m]$ and the $(N \times d^{\bar{u}})$ -matrices X^0 , $Y^{\bar{u}}$ for $\bar{u} \in \{0, e_1, \dots, e_m\}$, where

$$X^{e_i} := [\Phi(x_1^{e_i}) \quad \dots \quad \Phi(x_{d^{\bar{u}}}^{e_i})], \quad (12a)$$

$$X^0 := \begin{bmatrix} \begin{bmatrix} \phi_1(x_1^0) \\ \vdots \\ \phi_N(x_1^0) \end{bmatrix} & \dots & \begin{bmatrix} \phi_1(x_{d^0}^0) \\ \vdots \\ \phi_N(x_{d^0}^0) \end{bmatrix} \end{bmatrix}, \quad (12b)$$

$$Y^{\bar{u}} := \begin{bmatrix} \begin{bmatrix} (\mathcal{L}^{\bar{u}} \phi_1)(x_1^{\bar{u}}) \\ \vdots \\ (\mathcal{L}^{\bar{u}} \phi_N)(x_1^{\bar{u}}) \end{bmatrix} & \dots & \begin{bmatrix} (\mathcal{L}^{\bar{u}} \phi_1)(x_{d^{\bar{u}}}^{\bar{u}}) \\ \vdots \\ (\mathcal{L}^{\bar{u}} \phi_N)(x_{d^{\bar{u}}}^{\bar{u}}) \end{bmatrix} \end{bmatrix}, \quad (12c)$$

with

$$\begin{aligned} (\mathcal{L}^{\bar{u}} \phi_k)(x_j^{\bar{u}}) &= \nabla \phi_k(x_j^{\bar{u}})^\top \left(f(x_j^{\bar{u}}) + \sum_{i=1}^m g_i(x_j^{\bar{u}}) \bar{u} \right) \\ &= \nabla \phi_k(x_j^{\bar{u}})^\top \hat{x}_j^{\bar{u}} \end{aligned} \quad (13)$$

for $k \in [N]$ and $j \in [d^{\bar{u}}]$. Then, the generator EDMD-based surrogate for the Koopman generator $P_{\mathbb{V}} \mathcal{L}^{\bar{u}}|_{\mathbb{V}}$ is given by

$$\mathcal{L}_d^0 = \begin{bmatrix} 0 & 0_{1 \times N} \\ 0_{N \times 1} & A \end{bmatrix}, \quad \mathcal{L}_d^{e_i} = \begin{bmatrix} 0 & 0_{1 \times N} \\ B_{0,i} & \hat{B}_i \end{bmatrix} \quad (14)$$

for $i \in [m]$, where

$$A = \arg \min_{A \in \mathbb{R}^{N \times N}} \|Y^0 - AX^0\|_{\mathbb{F}}, \quad (15a)$$

$$[B_{0,i} \quad \hat{B}_i] = \arg \min_{\substack{B_{0,i} \in \mathbb{R}^N, \\ \hat{B}_i \in \mathbb{R}^{N \times N}}} \|Y^{e_i} - [B_{0,i} \quad \hat{B}_i] X^{e_i}\|_{\mathbb{F}} \quad (15b)$$

for $i \in [m]$ and $\|\cdot\|_{\mathbb{F}}$ denotes the Frobenius norm. The explicit solutions to these problems read $A = Y^0(X^0)^\dagger$ and $[B_{0,i} \quad \hat{B}_i] = Y^{e_i}(X^{e_i})^\dagger$. Motivated by the control-affine structure of the Koopman generator (5), we define its data-based approximation as

$$\mathcal{L}_d^u = \mathcal{L}_d^0 + \sum_{i=1}^m u_i (\mathcal{L}_d^{e_i} - \mathcal{L}_d^0). \quad (16)$$

2) *EDMD error bounds*: The following proposition captures the error between the Koopman generator and its data-driven EDMD estimate.

Proposition 3 ([33, Thm. 3]). *Suppose that Assumption 2 holds and the data samples are i.i.d. Further, let an error bound $L_r > 0$ and a probabilistic tolerance $\delta \in (0, 1)$ be given. Then, there is an amount of data $d_0 \in \mathbb{N}$ such for all $d \geq d_0$ and all $u \in \mathbb{U}$ we have the error bound*

$$\|\mathcal{L}^u|_{\mathbb{V}} - \mathcal{L}_d^u\| \leq L_r \quad (17)$$

with probability $1 - \delta$.

The precise dependence of the sufficient amount of data d_0 was provided in [33, Thm. 3]. For given dictionary size $N+1$, $N \in \mathbb{N}$, probabilistic tolerance $\delta \in (0, 1)$ and error bound $L_r > 0$, we define

$$\tilde{\delta} := \frac{\delta}{3(m+1)} \in (0, 1) \quad (18)$$

$$\tilde{L}_r := \frac{L_r}{(m+1)(1 + \max_{u \in \mathbb{U}} \sum_{i=1}^m |u_i|)} > 0. \quad (19)$$

Then, for $k \in [0 : m]$, let the matrices $A^{(k)}, C \in \mathbb{R}^{(N+1) \times (N+1)}$ be defined by $(A^{(k)})_{i,j} = \langle \phi_i, \mathcal{L}^{e_k} \phi_j \rangle_{L^2(\mathbb{X})}$ and $C_{i,j} := \langle \phi_i, \phi_j \rangle_{L^2(\mathbb{X})}$ and set

$$\tilde{L}_{r,k} = \min \left\{ 1, \frac{1}{\|A^{(k)}\| \|C^{-1}\|} \right\} \cdot \frac{\|A^{(k)}\| \tilde{L}_r}{2\|A^{(k)}\| \|C^{-1}\| + \tilde{L}_r}.$$

Then, the sufficient number of data points $d_0 \in \mathbb{N}$ for the probabilistic bound of Proposition 3 is given by

$$d_0 \geq \max_{k=0, \dots, m} \frac{(N+1)^2}{\tilde{\delta} \tilde{L}_{r,k}^2} \max \{ \|\Sigma_{A^{(k)}}\|_F^2, \|\Sigma_C\|_F^2 \} \quad (20)$$

where $\Sigma_{A^{(k)}}$ and Σ_C are variance matrices defined via

$$\begin{aligned} (\Sigma_{A^{(k)}})_{i,j}^2 &= \frac{1}{|\mathbb{X}|} \int_{\mathbb{X}} \phi_i(x)^2 \langle \nabla \phi_j(x), f(x) + g_k(x) \rangle^2 dx \\ &\quad - \left(\frac{1}{|\mathbb{X}|} \int_{\mathbb{X}} \phi_i(x) \langle \nabla \phi_j(x), f(x) + g_k(x) \rangle dx \right)^2 \end{aligned}$$

and

$$\begin{aligned} (\Sigma_C)_{i,j}^2 &= \frac{1}{|\mathbb{X}|} \int_{\mathbb{X}} \phi_i(x)^2 \phi_j(x)^2 dx \\ &\quad - \left(\frac{1}{|\mathbb{X}|} \int_{\mathbb{X}} \phi_i(x) \phi_j(x) dx \right)^2 \end{aligned}$$

for $(i, j) \in [N+1]^2$ and where $|\mathbb{X}|$ denotes the Lebesgue measure of \mathbb{X} .

In the following, we omit the initial value and the control argument and abbreviate $x(t) = x(t; \hat{x}, u)$. Using the Koopman generator, the observables along the nonlinear dynamics (1) satisfy

$$\begin{aligned} \frac{d}{dt} \Phi(x(t)) &= \mathcal{L}^u \Phi(x(t)) \\ &= \mathcal{L}_d^u \Phi(x(t)) + (\mathcal{L}^u - \mathcal{L}_d^u) \Phi(x(t)). \end{aligned} \quad (21)$$

Thus, the dynamics along the data-driven surrogate \mathcal{L}_d^u can be interpreted as a perturbed version of the original lifted dynamics with the remainder

$$\begin{aligned} r(x, u) &= (\mathcal{L}^u - \mathcal{L}_d^u)\Phi(x) \\ &= (\mathcal{L}^u - \mathcal{L}_d^u)(\Phi(x) - \Phi(0) + \Phi(0)), \end{aligned} \quad (22)$$

which in view of Proposition 3 satisfies the bound

$$\|r(x, u)\| \leq L_r(\|\Phi(x) - \Phi(0)\| + \|\Phi(0)\|) \quad (23)$$

for all $x \in \mathbb{X}$ and $u \in \mathbb{U}$ with probability $1 - \delta$.

This error bound, however, has a significant drawback in view of controller design: The upper bound contains a state-independent part and thus, as $\Phi(0) \neq 0$ due to the constant observable, it does not vanish for $x = 0$ and $u = 0$, which is the targeted equilibrium point of the dynamics. To address this issue by means of an alternative (and *proportional*) error bound, we adapt the line of reasoning of [42, Prop. 8] leading to new error estimates for the compression of the Koopman generator in the lifted space, which guarantees that the residual vanishes at the origin, i.e., $r(x, u) = 0$ for $x = 0$ and $u = 0$. To this end, we define the reduced lifted state

$$\hat{\Phi}(x) = \begin{bmatrix} 0_{N \times 1} & I_N \end{bmatrix} \Phi(x) \quad (24)$$

which allows the characterization of the lifted dynamics with a proportional error bound on the remainder as follows.

Lemma 4. *The lifted dynamics (21) are equivalently captured by*

$$\begin{aligned} \frac{d}{dt} \hat{\Phi}(x(t)) &= A \hat{\Phi}(x(t)) + B_0 u(t) \\ &+ \sum_{i=1}^m u_i(t) B_i \hat{\Phi}(x(t)) + \hat{r}(x(t), u(t)), \end{aligned} \quad (25)$$

where $B_0 = [B_{0,1} \ \cdots \ B_{0,m}]$, $B_i = \hat{B}_i - A$. Then, the remainder is bounded by

$$\|\hat{r}(x, u)\| \leq L_r(\|\hat{\Phi}(x)\| + \|u\|) \quad (26)$$

for all $(x, u) \in \mathbb{X} \times \mathbb{U}$ with probability $1 - \delta$.

Proof. Let $(x, u) \in \mathbb{X} \times \mathbb{U}$. The structure of the Koopman generators (11) ensures

$$\begin{aligned} (\mathcal{L}^0 \Phi)(x) &= \begin{bmatrix} 0 \\ (\mathcal{L}_{22}^0 \hat{\Phi})(x) \end{bmatrix}, \\ (\mathcal{L}^{e_i} \Phi)(x) &= \begin{bmatrix} 0 \\ \mathcal{L}_{21}^{e_i} + (\mathcal{L}_{22}^{e_i} \hat{\Phi})(x) \end{bmatrix}, \quad i \in [m]. \end{aligned}$$

By defining $\mathcal{L}_{21}^e = [\mathcal{L}_{21}^{e_1} \ \cdots \ \mathcal{L}_{21}^{e_m}]$ and $\tilde{\mathcal{L}}_{22}^{e_i} = \mathcal{L}_{22}^{e_i} - \mathcal{L}_{22}^0$ we deduce

$$(\mathcal{L}^u \Phi)(x) = \begin{bmatrix} 0 \\ (\mathcal{L}_{22}^0 \hat{\Phi})(x) + \mathcal{L}_{21}^e u + \sum_{i=1}^m u_i (\tilde{\mathcal{L}}_{22}^{e_i} \hat{\Phi})(x) \end{bmatrix}.$$

Due to (14) the same structure applies for the corresponding EDMD approximation, i.e.,

$$\mathcal{L}_d^u \Phi(x) = \begin{bmatrix} 0 \\ A \hat{\Phi}(x) + B_0 u + \sum_{i=1}^m u_i B_i \hat{\Phi}(x) \end{bmatrix} \quad (27)$$

with $B_0 = [B_{0,1} \ \cdots \ B_{0,m}]$ and $B_i = \hat{B}_i - A$. Since $\hat{\Phi}(0) = 0$ holds, $(\mathcal{L}^u - \mathcal{L}_d^u)\Phi(0) = \begin{bmatrix} 0 \\ (\mathcal{L}_{21}^e - B_0)u \end{bmatrix}$ such that

$$\|(\mathcal{L}^u - \mathcal{L}_d^u)\Phi(0)\| \leq \|\mathcal{L}_{21}^e - B_0\| \|u\|. \quad (28)$$

Moreover, by construction, the first row of the remainder $r(x, u)$ in (21) vanishes, i.e.,

$$r(x, u) = (\mathcal{L}^u - \mathcal{L}_d^u)\Phi(x) = \begin{bmatrix} 0 \\ \hat{r}(x, u) \end{bmatrix}, \quad (29)$$

which implies that the first row of the right-hand side of (21) vanishes. Together with the vanishing derivative of the constant function along the flow, i.e., $\frac{d}{dt} \phi_0(x(t)) \equiv 0$, this yields (25) when omitting the trivial first line. Finally, we observe $\Phi(x) - \Phi(0) = \begin{bmatrix} 0 \\ \hat{\Phi}(x) \end{bmatrix}$ and conclude

$$\begin{aligned} \|\hat{r}(x, u)\| &= \|r(x, u)\| \\ &\stackrel{(22)}{\leq} \|\mathcal{L}^u - \mathcal{L}_d^u\| \|\Phi(x) - \Phi(0)\| + \|(\mathcal{L}^u - \mathcal{L}_d^u)\Phi(0)\| \\ &\stackrel{(28)}{\leq} \|\mathcal{L}^u - \mathcal{L}_d^u\| \|\Phi(x) - \Phi(0)\| + \|\mathcal{L}_{21}^e - B_0\| \|u\|. \end{aligned} \quad (30)$$

Further, as $e_i \in \mathbb{U}$ for all $i \in [m]$, then the estimate in (17) not only bounds $\|\mathcal{L}^u - \mathcal{L}_d^u\|$ but yields also the (conservative) upper bound

$$\|\mathcal{L}_{21}^e - B_0\| = \|(\mathcal{L}^u - \mathcal{L}_d^u)\Phi(0)\| \leq \|\mathcal{L}^u - \mathcal{L}_d^u\| \|\Phi(0)\| \leq L_r.$$

Hence, invoking the bound on $\|\mathcal{L}^u - \mathcal{L}_d^u\|$ of Proposition 3 yields the claim. \square

Lemma 4 establishes a finite-dimensional bilinear representation of the nonlinear system (1), where the remainder is bounded via the norm of the lifted state $\hat{\Phi}(x)$ and the input u . Due to the construction of $\hat{\Phi}$, this removes the constant offset at the origin $x = 0$ occurring in the error bound (23) and allows convex data-driven controller design for the nonlinear system (1). We note that, as becomes clear from the last part of the proof of Lemma 4, the constant appearing with the control value u in (26) can be tightened further by exploiting the derivation of (17), which is left for future research.

For the remainder of the paper, we will omit the time argument for the ease of notation, wherever it is clear from the context.

III. DATA-DRIVEN CONTROL OF NONLINEAR SYSTEMS

In this section, we develop a controller for the nonlinear system (1) based on the data-driven Koopman representation derived in Section II-B. We provide a tutorial-style exposition of the derivation in a simplified setting with single-input systems and state-feedback controllers that depend linearly on the lifted state $\hat{\Phi}(x)$, i.e., $\mu(x) = K \hat{\Phi}(x)$ holds with a matrix $K \in \mathbb{R}^{1 \times N}$. Section III-A introduces a reformulation of the corresponding lifted system dynamics as a robust linear control problem. Then, we use convex optimization to solve the control problem in Section III-B. The case with multi-input systems and more general controller parametrizations will be considered in Section IV.

A. Reformulation as robust linear control problem

First, we recall the lifted system dynamics (25) for scalar inputs ($m = 1$), i.e.,

$$\frac{d}{dt}\hat{\Phi}(x) = A\hat{\Phi}(x) + B_0u + B_1\hat{\Phi}(x)u + \hat{r}(x, u), \quad (31)$$

where the nonlinear remainder $\hat{r}(x, u)$ is bounded by the proportional bound (26) on $\mathbb{X} \times \mathbb{U}$. Our goal is to design a state-feedback controller $u = \mu(x)$ such that the origin of the closed-loop system is exponentially stable. To this end, we view (31) as an uncertain bilinear system, where the uncertainty is given by $\hat{r}(x, u)$. To cope with the uncertainty, we employ linear robust control techniques enabling methods from convex optimization. First, we treat the remainder in the lifted dynamics (25) as uncertainty and stabilize the system robustly using that $\hat{r}(x, u)$ satisfies the error bound (26) for all $x \in \mathbb{X}, u \in \mathbb{U}$. To this end, we define the remainder $\varepsilon : \mathbb{R}^N \times \mathbb{R}^m \rightarrow \mathbb{R}^N$ depending on the lifted state as

$$\varepsilon(v_1, v_2) = \hat{r} \left(\begin{bmatrix} I_n & 0_{n \times N-n} \end{bmatrix} v_1, v_2 \right). \quad (32)$$

According to (26), ε satisfies also a proportional bound, i.e.,

$$\|\varepsilon(\hat{\Phi}(x), u)\| = \|\hat{r}(x, u)\| \leq L_r(\|\hat{\Phi}(x)\| + \|u\|) \quad (33)$$

for all $x \in \mathbb{X}, u \in \mathbb{U}$. Second, we introduce an additional uncertainty Δ_Φ corresponding to the term $\hat{\Phi}(x)$. To this end, we need to ensure that x and, in particular, $\hat{\Phi}(x)$ are bounded. Thus, we introduce an a priori fixed set Δ_Φ of the form $\Delta_\Phi := \{\Delta_\Phi \in \mathbb{R}^N \mid (34) \text{ holds}\}$ with

$$\begin{bmatrix} \Delta_\Phi \\ 1 \end{bmatrix}^\top \begin{bmatrix} Q_z & S_z \\ S_z^\top & R_z \end{bmatrix} \begin{bmatrix} \Delta_\Phi \\ 1 \end{bmatrix} \geq 0 \quad (34)$$

for fixed matrices $Q_z \in \mathbb{R}^{N \times N}$, $S_z \in \mathbb{R}^N$, $R_z \in \mathbb{R}$ with $Q_z \prec 0$ and $R_z > 0$ for which the inverse

$$\begin{bmatrix} \tilde{Q}_z & \tilde{S}_z \\ \tilde{S}_z^\top & \tilde{R}_z \end{bmatrix} := \begin{bmatrix} Q_z & S_z \\ S_z^\top & R_z \end{bmatrix}^{-1}$$

exists. The parametrization (34) of Δ_Φ includes, e.g., a region described by $\Delta_\Phi^\top \Delta_\Phi \leq c$ with $c > 0$ when choosing $Q_z = -I$, $S_z = 0$, and $R_z = c$. Our later derived controller design will ensure that the closed-loop system satisfies $\hat{\Phi}(x(t)) \in \Delta_\Phi$ for all t . More precisely, we stabilize the bilinear system (31) by robustly stabilizing

$$\frac{d}{dt}\hat{\Phi}(x) = A\hat{\Phi}(x) + B_0u + B_1\Delta_\Phi u + \varepsilon(\hat{\Phi}(x), u) \quad (35)$$

for all $\Delta_\Phi \in \Delta_\Phi$ and perturbation functions ε satisfying (33) for all $x \in \mathbb{X}, u \in \mathbb{U}$.

Now, we write the lifted system described by the uncertain bilinear system (31) using a linear fractional representation (LFR). In particular, we consider the LFR corresponding to (35) given by

$$\begin{bmatrix} \frac{d}{dt}\hat{\Phi}(x) \\ u \\ \begin{bmatrix} v_1 \\ v_2 \end{bmatrix} \end{bmatrix} = \begin{bmatrix} A & B_0 & B_1 & I \\ 0 & I & 0 & 0 \\ \begin{bmatrix} I \\ 0 \end{bmatrix} & \begin{bmatrix} 0 \\ I \end{bmatrix} & 0 & 0 \end{bmatrix} \begin{bmatrix} \hat{\Phi}(x) \\ u \\ w_\Phi \\ w_r \end{bmatrix}, \quad (36a)$$

$$w_\Phi = \Delta_\Phi u, \quad (36b)$$

$$w_r = \varepsilon(v_1, v_2) \quad (36c)$$

with $\Delta_\Phi \in \Delta_\Phi$ and ε satisfying (33) for all $x \in \mathbb{X}, u \in \mathbb{U}$. An LFR as in (36) is a common representation of uncertain systems [57]. Here, the LFR is exposed to two uncertainties, where we reduce the bilinear control problem to a linear control problem subject to an unknown state-dependent nonlinearity, i.e., the (known) lifted state $\Delta_\Phi = \hat{\Phi}(x)$, and the nonlinearity $\varepsilon(\hat{\Phi}(x), u)$ corresponding to the (unknown) remainder $\hat{r}(x, u)$. Note that the LFR (36) is highly structured with several zero terms and, thus, the dynamics depend linearly on the uncertainties. However, we note that the LFR framework offers the possibility to adapt the subsequent analysis to more general (fractional) uncertainty descriptions in future work.

B. Solution via linear matrix inequalities

In the following, we design a state-feedback controller that is linear in the lifted state, i.e., $\mu(x) = K\hat{\Phi}(x)$ for some $K \in \mathbb{R}^{1 \times N}$. Setting $A_K = A + B_0K$ and substituting the input by the feedback in the open-loop LFR (36), we obtain the corresponding closed-loop LFR

$$\begin{bmatrix} \frac{d}{dt}\hat{\Phi}(x) \\ \mu(x) \\ \begin{bmatrix} v_1 \\ v_2 \end{bmatrix} \end{bmatrix} = \begin{bmatrix} A_K & B_1 & I \\ K & 0 & 0 \\ \begin{bmatrix} I \\ K \end{bmatrix} & 0 & 0 \end{bmatrix} \begin{bmatrix} \hat{\Phi}(x) \\ w_\Phi \\ w_r \end{bmatrix}, \quad (37a)$$

$$w_\Phi = \Delta_\Phi \mu(x), \quad (37b)$$

$$w_r = \varepsilon(v_1, v_2) \quad (37c)$$

with $\Delta_\Phi \in \Delta_\Phi$ and ε satisfying (33) for all $x \in \mathbb{X}, u \in \mathbb{U}$.

The following theorem establishes a controller design method guaranteeing exponential stability for the nonlinear system (1) by solving an LMI feasibility problem.

Theorem 5. *Let Assumption 2 hold. Suppose a desired error bound $L_r > 0$ and a probabilistic tolerance $\delta \in (0, 1)$ in the sense of Proposition 3 are given. If there exist a matrix $0 \prec P = P^\top \in \mathbb{R}^{N \times N}$, a matrix $L \in \mathbb{R}^{1 \times N}$, and scalars $\lambda > 0$, $\nu > 0$, $\tau > 0$ such that (38) and*

$$\begin{bmatrix} P & PS_z & P & 0 \\ S_z^\top P & \nu R_z & 0 & \nu \\ P & 0 & -\nu Q_z^{-1} & 0 \\ 0 & \nu & 0 & 1 \end{bmatrix} \succeq 0 \quad (39)$$

hold, then there exists an amount of data $d_0 \in \mathbb{N}$ such that for all $d \geq d_0$ the controller $\mu(x) = LP^{-1}\hat{\Phi}(x)$ achieves exponential stability of the nonlinear system (1) for all initial conditions $\hat{x} \in \mathcal{X}_{\text{RoA}} := \{x \in \mathbb{R}^n \mid \hat{\Phi}(x)^\top P^{-1}\hat{\Phi}(x) \leq 1\}$ with probability $1 - \delta$.

Proof. We divide the proof into two parts, where we first show that all $x \in \mathcal{X}_{\text{RoA}}$ satisfy $\hat{\Phi}(x) \in \Delta_\Phi$ and then conclude positive invariance of \mathcal{X}_{RoA} together with exponential stability of the closed-loop system (2) for all $\hat{x} \in \mathcal{X}_{\text{RoA}}$.

Part I: $x \in \mathcal{X}_{\text{RoA}}$ implies $\hat{\Phi}(x) \in \Delta_\Phi$: The presented representation of the nonlinear system as an LFR (37) requires $\hat{\Phi}(x) \in \Delta_\Phi$. Thus, first observe that (39) is equivalent to

$$\begin{bmatrix} \frac{1}{\nu}P & \frac{1}{\nu}PS_z \\ \frac{1}{\nu}S_z^\top P & R_z \end{bmatrix} + \begin{bmatrix} \frac{1}{\nu}P \\ 0 \end{bmatrix} Q_z \begin{bmatrix} \frac{1}{\nu}P \\ 0 \end{bmatrix}^\top - \begin{bmatrix} 0 \\ 1 \end{bmatrix} \nu \begin{bmatrix} 0 \\ 1 \end{bmatrix}^\top \succeq 0,$$

$$\begin{bmatrix} -AP - B_0L - PA^\top - L^\top B_0^\top - \tau I_N & -L^\top - \lambda B_1 \tilde{S}_z & -[P \ L^\top] & \lambda B_1 \\ & -L - \lambda \tilde{S}_z^\top B_1^\top & \lambda \tilde{R}_z & 0 \\ & [P \ L^\top]^\top & 0 & 0.5\tau L_r^{-2} I_{N+1} \\ & \lambda B_1^\top & 0 & 0 \\ & & & -\lambda \tilde{Q}_z^{-1} \end{bmatrix} \succ 0 \quad (38)$$

where we first divide the inequality by ν and then apply the Schur complement (cf. [58]) twice. Multiplying from the left and from the right by $\text{diag}(\nu P^{-1}, 1)$ yields

$$\begin{bmatrix} Q_z & S_z \\ S_z^\top & R_z \end{bmatrix} - \nu \begin{bmatrix} -P^{-1} & 0 \\ 0 & 1 \end{bmatrix} \succeq 0.$$

Multiplying from left and right by $[\hat{\Phi}(x)^\top \ 1]^\top$ and its transpose, respectively, where $x \in \mathcal{X}_{\text{RoA}}$, results in $\hat{\Phi}(x) \in \Delta_\Phi$ for all $x \in \mathcal{X}_{\text{RoA}}$ (cf. the S-procedure [58], [59]), where Δ_Φ is defined in (34).

Part II: Positive invariance of \mathcal{X}_{RoA} and exponential stability: For positive invariance of \mathcal{X}_{RoA} , we have to show that $x(t + \chi) \in \mathcal{X}_{\text{RoA}}$ for all $x(t) \in \mathcal{X}_{\text{RoA}}$ and $\chi > 0$. According to the definition of \mathcal{X}_{RoA} , we define the Lyapunov function candidate $V(x) = \hat{\Phi}(x)^\top P^{-1} \hat{\Phi}(x)$ such that positive invariance follows if $\frac{d}{dt} V(x(t)) \leq 0$ for all trajectories satisfying $x(t) \in \mathcal{X}_{\text{RoA}}$, $t \geq 0$.

First, we define $K = LP^{-1}$ and recall $A_K = A + B_0K$. Then, we apply the Schur complement to (38) to obtain

$$\begin{bmatrix} -A_K P - P A_K^\top - \tau I_N & \star & \star \\ -KP - \lambda \tilde{S}_z^\top B_1^\top & \lambda \tilde{R}_z & \star \\ -\begin{bmatrix} P \\ KP \end{bmatrix} & 0 & 0.5\tau L_r^{-2} I_{N+1} \end{bmatrix} + \lambda^{-1} \begin{bmatrix} \lambda B_1 \\ 0 \\ 0 \end{bmatrix} \tilde{Q}_z \begin{bmatrix} \lambda B_1 \\ 0 \\ 0 \end{bmatrix}^\top \succ 0. \quad (40)$$

Note that

$$\begin{bmatrix} -A_K P - P A_K^\top & \star & \star \\ -KP & 0 & \star \\ -\begin{bmatrix} P \\ KP \end{bmatrix} & 0 & 0 \end{bmatrix} = \begin{bmatrix} A_K & -I \\ K & 0 \\ I & 0 \\ K & 0 \end{bmatrix} \begin{bmatrix} 0 & P \\ P & 0 \end{bmatrix} [\star]^\top \quad (41)$$

and

$$\begin{bmatrix} 0 & -\lambda B_1 \tilde{S}_z & 0 \\ \star & \lambda \tilde{R}_z & 0 \\ \star & \star & 0 \end{bmatrix} + \lambda \begin{bmatrix} B_1 \\ 0 \\ 0 \end{bmatrix} \tilde{Q}_z \begin{bmatrix} B_1 \\ 0 \\ 0 \end{bmatrix}^\top = \lambda \begin{bmatrix} B_1 & 0 \\ 0 & -I \\ 0 & 0 \end{bmatrix} \begin{bmatrix} \tilde{Q}_z & \tilde{S}_z \\ \tilde{S}_z^\top & \tilde{R}_z \end{bmatrix} \begin{bmatrix} B_1 & 0 \\ 0 & -I \\ 0 & 0 \end{bmatrix}^\top.$$

Moreover, we define

$$\Pi_r = \begin{bmatrix} -I_N & 0 \\ 0 & 2L_r^2 I_{N+m} \end{bmatrix}, \quad \Pi_r^{-1} = \begin{bmatrix} -I_N & 0 \\ 0 & 0.5L_r^{-2} I_{N+m} \end{bmatrix}, \quad (42)$$

to obtain

$$\begin{bmatrix} -\tau I_N & 0 & 0 \\ 0 & 0 & 0 \\ 0 & 0 & 0.5\tau L_r^{-2} I_{N+1} \end{bmatrix} = \tau \begin{bmatrix} I & 0 \\ 0 & 0 \\ 0 & -I \end{bmatrix} \Pi_r^{-1} [\star]^\top. \quad (43)$$

Thus, we write (40) equivalently as

$$\Psi^\top \text{diag} \left(\begin{bmatrix} 0 & P \\ P & 0 \end{bmatrix}, \lambda \begin{bmatrix} \tilde{Q}_z & \tilde{S}_z \\ \tilde{S}_z^\top & \tilde{R}_z \end{bmatrix}, \tau \Pi_r^{-1} \right) \Psi \succ 0, \quad (44)$$

where

$$\Psi^\top = \begin{bmatrix} A_K & -I & B_1 & 0 & I & 0 \\ K & 0 & 0 & -I & 0 & 0 \\ I & 0 & 0 & 0 & 0 & -I \\ K & 0 & 0 & 0 & 0 & -I \end{bmatrix}. \quad (45)$$

Then, we apply the dualization lemma [59, Lm. 4.9] to arrive at

$$\tilde{\Psi}^\top \text{diag} \left(\begin{bmatrix} 0 & \tilde{P} \\ \tilde{P} & 0 \end{bmatrix}, \lambda^{-1} \begin{bmatrix} Q_z & S_z \\ S_z^\top & R_z \end{bmatrix}, \tau^{-1} \Pi_r \right) \tilde{\Psi} \succ 0, \quad (46)$$

where $\tilde{P} = P^{-1}$ and

$$\tilde{\Psi}^\top = \begin{bmatrix} I & A_K^\top & 0 & K^\top & 0 & I & K^\top \\ 0 & B_1^\top & I & 0 & 0 & 0 & 0 \\ 0 & I & 0 & 0 & I & 0 & 0 \end{bmatrix} \quad (47)$$

is constructed similarly to the discussion in [59, Sec. 8.1.2]. By multiplying (46) from the left and from the right by $[\hat{\Phi}(x)^\top \ \mu(x) \Delta_\Phi^\top \ \varepsilon(\hat{\Phi}(x), \mu(x))^\top]^\top$ and its transpose, respectively, where $x \in \mathcal{X}_{\text{RoA}}$, $\mu(x) = K\hat{\Phi}(x)$, $\Delta_\Phi \in \Delta_\Phi$, and $\varepsilon(\hat{\Phi}(x), \mu(x))$ satisfies (33), we obtain

$$\begin{aligned} & [\star]^\top \begin{bmatrix} 0 & \tilde{P} \\ \tilde{P} & 0 \end{bmatrix} \begin{bmatrix} \hat{\Phi}(x) \\ A_K \hat{\Phi}(x) + B_1 \Delta_\Phi \mu(x) + \varepsilon(\hat{\Phi}(x), \mu(x)) \end{bmatrix} \\ & + \lambda^{-1} [\star]^\top \begin{bmatrix} Q_z & S_z \\ S_z^\top & R_z \end{bmatrix} \begin{bmatrix} \Delta_\Phi \mu(x) \\ K \hat{\Phi}(x) \end{bmatrix} \\ & + \tau^{-1} [\star]^\top \Pi_r \begin{bmatrix} \varepsilon(\hat{\Phi}(x), \mu(x)) \\ \hat{\Phi}(x) \\ K \hat{\Phi}(x) \end{bmatrix} < 0. \quad (48) \end{aligned}$$

For $\Delta_\Phi \in \Delta_\Phi$ and $\varepsilon(\hat{\Phi}(x), \mu(x))$ satisfying (33), the last two summands of (48) are nonnegative as

$$\mu(x)^2 \begin{bmatrix} \Delta_\Phi \\ 1 \end{bmatrix}^\top \begin{bmatrix} Q_z & S_z \\ S_z^\top & R_z \end{bmatrix} \begin{bmatrix} \Delta_\Phi \\ 1 \end{bmatrix} \geq 0$$

with the definition of Δ_Φ in (34) and

$$\begin{aligned} & [\star]^\top \Pi_r \begin{bmatrix} \varepsilon(\hat{\Phi}(x), \mu(x)) \\ \hat{\Phi}(x) \\ K \hat{\Phi}(x) \end{bmatrix} \\ & = 2L_r^2 (\|\hat{\Phi}(x)\|^2 + \|\mu(x)\|^2) - \|\varepsilon(\hat{\Phi}(x), \mu(x))\|^2 \\ & \geq L_r^2 (\|\hat{\Phi}(x)\| + \|\mu(x)\|)^2 - \|\varepsilon(\hat{\Phi}(x), \mu(x))\|^2 \geq 0. \end{aligned}$$

Hence, (48) implies

$$\begin{aligned} 0 & > \hat{\Phi}(x)^\top \tilde{P} (A_K \hat{\Phi}(x) + B_1 \Delta_\Phi \mu(x) + \varepsilon(\hat{\Phi}(x), \mu(x))) \\ & + (A_K \hat{\Phi}(x) + B_1 \Delta_\Phi \mu(x) + \varepsilon(\hat{\Phi}(x), \mu(x)))^\top \tilde{P} \hat{\Phi}(x) \quad (49) \end{aligned}$$

if $x \in \mathcal{X}_{\text{RoA}} \setminus \{0\}$, $\Delta_\Phi \in \mathbf{\Delta}_\Phi$, and if $\varepsilon(\hat{\Phi}(x), \mu(x))$ satisfies (33) (again, we refer to the S-procedure [58], [59]).

Recall the Lyapunov candidate function $V(x) = \hat{\Phi}(x)^\top \tilde{P} \hat{\Phi}(x)$ which satisfies $V(0) = 0$ and

$$V(x) \leq \sigma_{\max}(\tilde{P}) \|\hat{\Phi}(x)\|^2 \leq \sigma_{\max}(\tilde{P}) L_\Phi^2 \|x\|^2, \quad (50a)$$

$$V(x) \geq \sigma_{\min}(\tilde{P}) \|\hat{\Phi}(x)\|^2 \geq \sigma_{\min}(\tilde{P}) \|x\|^2 \quad (50b)$$

due to $\|\hat{\Phi}(x)\| = \|\Phi(x) - \Phi(0)\|$, (7), and (8). Further, substituting $\frac{d}{dt} \hat{\Phi}(x(t)) = A_K \hat{\Phi}(x(t)) + B_1 \Delta_\Phi(t) \mu(x(t)) + \varepsilon(\hat{\Phi}(x), \mu(x))$ in (49) leads to

$$\begin{aligned} \frac{d}{dt} V(x(t)) &= \hat{\Phi}(x(t))^\top \tilde{P} \left(\frac{d}{dt} \hat{\Phi}(x(t)) \right) \\ &\quad + \left(\frac{d}{dt} \hat{\Phi}(x(t)) \right)^\top \tilde{P} \hat{\Phi}(x(t)) < 0 \end{aligned} \quad (51)$$

if $x(t) \in \mathcal{X}_{\text{RoA}} \setminus \{0\}$, $\Delta_\Phi(t) \in \mathbf{\Delta}_\Phi$, and if $\varepsilon(\hat{\Phi}(x), \mu(x))$ satisfies (33). Hence, the controller $\mu(x(t)) = K \hat{\Phi}(x(t))$ guarantees the decrease (51) for solutions of the LFR (37) and, thus, also for the lifted system (35) if $x(t) \in \mathcal{X}_{\text{RoA}} \setminus \{0\}$, $\Delta_\Phi(t) \in \mathbf{\Delta}_\Phi$, and if $\varepsilon(\hat{\Phi}(x(t)), \mu(x(t)))$ satisfies (33). Recall that $\hat{\Phi}(x(t)) \in \mathbf{\Delta}_\Phi$ for all $x(t) \in \mathcal{X}_{\text{RoA}}$ according to Part I and $\varepsilon(\hat{\Phi}(x(t)), \mu(x(t))) = \hat{r}(x(t), u(t))$ due to (32). Thus, the controller $\mu(x(t)) = K \hat{\Phi}(x(t))$ guarantees (51) in particular for system (31) for all $x(t) \in \mathcal{X}_{\text{RoA}} \setminus \{0\}$ if $\hat{r}(x(t), \mu(x(t)))$ satisfies (26). This concludes positive invariance of \mathcal{X}_{RoA} and, thus, robust exponential stability of (31) for all $x(t) \in \mathcal{X}_{\text{RoA}}$ if $\hat{r}(x(t), \mu(x(t)))$ satisfies (26). Finally, we exploit Proposition 3 and Lemma 4 to deduce that the lifted system based on the data-driven approximation \mathcal{L}_d^u of the Koopman generator and its remainder $\hat{r}(x(t), \mu(x(t)))$ for a data length $d \geq d_0$ satisfies the obtained bound with probability $1 - \delta$. Hence, we conclude exponential stability of the nonlinear system (1) for all $x(t) \in \mathcal{X}_{\text{RoA}}$ with probability $1 - \delta$. \square

Theorem 5 establishes a robust controller design w.r.t. two uncertainties, namely the uncertain remainder $\hat{r}(x, u)$ and the (artificial) uncertainty $\Phi(x)$ which are both bounded. We emphasize that the controller design relies on an SDP in terms of LMIs which can be efficiently solved. The design of this robust controller is based on the sampling error bounds derived in [33]. In particular, the contributions of the presented controller design are the obtained closed-loop guarantees for the unknown nonlinear system (1) based on data. We note that our controller design exploits the fact that the control input also enters state-independently into the lifted dynamics via B_0 . More precisely, (38) can only be feasible if (A, B_0) is stabilizable.

A key technical ingredient of the proof is to derive Lyapunov stability directly for the *true* nonlinear system instead of restricting it to the lifted bilinear system. Thus, the considered error bound based on the Koopman approximation can be directly used when proving closed-loop stability of the nonlinear system (1) without additional consideration of the resulting submanifold $\text{im}(\hat{\Phi})$ resulting by the chosen lifting, cf. [45]. In addition, the tutorial-style presentation and proof of Theorem 5 contribute to a comprehensive controller design that can be widely used in various disciplines. Even though

Algorithm 1 State-feedback controller design for single inputs corresponding to Theorem 5.

Input:

- Data $\{x_j^{\bar{u}}, \hat{x}_j^{\bar{u}}\}_{j=1}^{d^{\bar{u}}}$ for $\bar{u} \in \{0, 1\}$, where $d^{\bar{u}} \geq d_0$ for d_0 according to (20)
- Lifting $\Phi(x) = [1 \ \hat{\Phi}(x)]^\top$ defined in (6) satisfies Assumption 2
- Probabilistic tolerance $\delta \in (0, 1)$ and error bound $L_r > 0$
- Ellipsoidal region $\mathbf{\Delta}_\Phi$ defined by $Q_z \prec 0, S_z, R_z > 0$

Output: Controller $u = \mu(x)$ for the nonlinear system (1) which is exponentially stabilizing with probability $1 - \delta$ if $\hat{x} \in \mathcal{X}_{\text{RoA}}$

Data-driven system representation:

Arrange the data according to (12) in $X^{\bar{u}}, Y^{\bar{u}}$

Solve the optimization problem (15) to obtain the data-based system matrices A, B_0, B_1 according to Lemma 4

Controller design:

Solve the LMI feasibility problem in Theorem 5

if successful then

Define the controller $\mu(x) = LP^{-1} \hat{\Phi}(x)$

end if

we only obtain probabilistic guarantees in Theorem 5, we exploit the direct relation between the necessary amount of data d_0 for a given desired accuracy of the lifting and certainty about the closed-loop guarantees presented in (20). Hence, the proposed controller design yields end-to-end guarantees for the underlying true nonlinear system (1) based on measured data.

The proposed controller design is summarized in Algorithm 1. Overall, we combine the EDMD estimate of the Koopman generator in (15) and the error bounds of Proposition 3 with the robust controller design in Theorem 5 leading to closed-loop guarantees of the nonlinear system (1).

Theorem 5 allows to compute state-feedback laws of the form $\mu(x) = K \hat{\Phi}(x)$ that stabilize nonlinear single-input systems. In Section IV (Theorem 6), we generalize this result into multiple directions. In particular, we exploit that the uncertainty signal w_Φ in (37) is, in fact, measurable during closed-loop operation given that $\Delta_\Phi = \hat{\Phi}(x)$ is known. This allows us to parametrize the controller as $\mu(x) = K \hat{\Phi}(x) + K_w w_\Phi$ for some matrix K_w . In contrast to Theorem 5, this yields a state feedback which depends nonlinearly on $\hat{\Phi}(x)$ as $\mu(x) = (I - K_w \hat{\Phi}(x))^{-1} K \hat{\Phi}(x)$. This more flexible controller structure provides less conservative stability conditions and, in general, a larger RoA \mathcal{X}_{RoA} than in Theorem 5. Further, we address the multi-input case.

IV. GENERAL STATE-FEEDBACK LAWS REDUCING CONSERVATISM

After presenting the main idea of the proposed controller design, we now discuss the design for general input dimensions ($m \geq 1$) and a more flexible controller structure reducing conservatism compared to the design in Section III.

To this end, we recall the lifted dynamics in (25) and define $\tilde{B} = [B_1 \ \cdots \ B_m]$ to compactly write the dynamics as

$$\frac{d}{dt}\hat{\Phi}(x) = A\hat{\Phi}(x) + B_0u + \tilde{B}(u \otimes \hat{\Phi}(x)) + \hat{r}(x, u). \quad (52)$$

Again, we impose that $\hat{\Phi}(x) \in \mathbf{\Delta}_\Phi$ with $\mathbf{\Delta}_\Phi$ defined prior to (34) and that the remainder $\hat{r}(x, u)$ satisfies (26) for all $x \in \mathbb{X}$ and $u \in \mathbb{U}$. Then, the lifted system (52) can be expressed as the open-loop LFR

$$\begin{bmatrix} \frac{d}{dt}\hat{\Phi}(x) \\ u \\ v_1 \\ v_2 \end{bmatrix} = \begin{bmatrix} A & B_0 & \tilde{B} & I \\ 0 & I & 0 & 0 \\ I & 0 & 0 & 0 \\ 0 & I & 0 & 0 \end{bmatrix} \begin{bmatrix} \hat{\Phi}(x) \\ u \\ w_\Phi \\ w_r \end{bmatrix}, \quad (53a)$$

$$w_\Phi = (I_m \otimes \Delta_\Phi)u, \quad (53b)$$

$$w_r = \varepsilon(v_1, v_2) \quad (53c)$$

with $\Delta_\Phi \in \mathbf{\Delta}_\Phi$ and ε as defined in (32) satisfying the bound (33) for all $x \in \mathbb{X}, u \in \mathbb{U}$. As main difference to (36), the LFR (53) is exposed to the uncertainty $(I_m \otimes \Delta_\Phi)$ instead of Δ_Φ . To derive an uncertainty characterization of $(I_m \otimes \Delta_\Phi)$, we define the set

$$\mathbf{\Delta} := \left\{ \Delta \in \mathbb{R}^{mN \times m} \left| \begin{bmatrix} \Delta \\ I \end{bmatrix}^\top \Pi_\Delta \begin{bmatrix} \Delta \\ I \end{bmatrix} \succeq 0 \ \forall \Pi_\Delta \in \mathbf{\Pi}_\Delta \right. \right\} \quad (54)$$

for some multiplier class $\mathbf{\Pi}_\Delta$ defined in the following as a suitable convex cone of symmetric matrices. More precisely, $\mathbf{\Pi}_\Delta$ needs to be chosen such that $(I_m \otimes \Delta_\Phi) \in \mathbf{\Delta}$ for all $\Delta_\Phi \in \mathbf{\Delta}_\Phi$. Thus, we parameterize the multiplier class via the LMI representation

$$\mathbf{\Pi}_\Delta := \left\{ \Pi_\Delta \left| \Pi_\Delta = \begin{bmatrix} \tilde{\Lambda} \otimes Q_z & \tilde{\Lambda} \otimes S_z \\ \tilde{\Lambda} \otimes S_z^\top & \tilde{\Lambda} \otimes R_z \end{bmatrix}, 0 \preceq \tilde{\Lambda} \in \mathbb{R}^{m \times m} \right. \right\}. \quad (55)$$

Using [43, Prop. 2], we deduce that $\Delta \in \mathbf{\Delta}$ if and only if $\Delta = I_m \otimes \Delta_\Phi$ with $\Delta_\Phi \in \mathbf{\Delta}_\Phi$. In particular, $\mathbf{\Delta}$ with multiplier class $\mathbf{\Pi}_\Delta$ exploits the structure of the uncertainty $\Delta = I_m \otimes \Delta_\Phi$ without additional conservatism. For scalar inputs, i.e., $m = 1$, the uncertainty description $\mathbf{\Delta}$ reduces to $\mathbf{\Delta}_\Phi$, i.e., $\mathbf{\Delta} = \mathbf{\Delta}_\Phi$.

In the following, we exploit that we can access the uncertainty $\Delta_\Phi = \hat{\Phi}(x)$ and, hence, $\Delta = I_m \otimes \hat{\Phi}(x)$ in the LFR channel (53b) by employing gain-scheduling techniques [60] to design a flexible state-feedback controller exponentially stabilizing the closed-loop. In particular, we design a full-information feedback controller [61]–[63] that depends not only on the lifted state $\hat{\Phi}(x)$ but also on the bilinearity $w_\Phi = \Delta u$. More precisely, we consider the feedback parametrization

$$u = \mu(x) = K\hat{\Phi}(x) + K_w w_\Phi, \quad (56)$$

where $K \in \mathbb{R}^{m \times N}$ and $K_w \in \mathbb{R}^{m \times Nm}$. Again, we abbreviate $A_K = A + B_0K$ and set $B_{K_w} = \tilde{B} + B_0K_w$. Substituting

(56) in the open-loop LFR (53), we obtain the corresponding closed-loop LFR

$$\begin{bmatrix} \frac{d}{dt}\hat{\Phi}(x) \\ \mu(x) \\ v_1 \\ v_2 \end{bmatrix} = \begin{bmatrix} A_K & B_{K_w} & I \\ K & K_w & 0 \\ I & 0 & 0 \\ K & K_w & 0 \end{bmatrix} \begin{bmatrix} \hat{\Phi}(x) \\ w_\Phi \\ w_r \end{bmatrix}, \quad (57a)$$

$$w_\Phi = \Delta\mu(x), \quad (57b)$$

$$w_r = \varepsilon(v_1, v_2) \quad (57c)$$

with $\Delta \in \mathbf{\Delta}$ and where ε satisfies (33) for all $x \in \mathbb{X}, u \in \mathbb{U}$. Note that the LFR (57) reduces to (37) in the case $m = 1$ and $K_w = 0$.

The following theorem establishes a controller design method guaranteeing exponential stability of the nonlinear system (1) based on robust exponential stability of the LFR (57).

Theorem 6. *Let Assumption 2 hold. Suppose a desired error bound $L_r > 0$ and a probabilistic tolerance $\delta \in (0, 1)$ in the sense of Proposition 3 are given. If there exists a matrix $0 \prec P = P^\top \in \mathbb{R}^{N \times N}$, matrices $L \in \mathbb{R}^{m \times N}$, $L_w \in \mathbb{R}^{m \times Nm}$, a matrix $0 \prec \Lambda = \Lambda^\top \in \mathbb{R}^{m \times m}$, and scalars $\nu > 0$, $\tau > 0$ such that (58) and*

$$\begin{bmatrix} P & PS_z & P & 0 \\ S_z^\top P & \nu R_z & 0 & \nu \\ P & 0 & -\nu Q_z^{-1} & 0 \\ 0 & \nu & 0 & 1 \end{bmatrix} \succeq 0 \quad (59)$$

hold, then there exists an amount of data $d_0 \in \mathbb{N}$ such that for all $d \geq d_0$ the controller

$$\mu(x) = (I - L_w(\Lambda^{-1} \otimes \hat{\Phi}(x)))^{-1}LP^{-1}\hat{\Phi}(x) \quad (60)$$

achieves exponential stability of the nonlinear system (1) for all initial conditions $\hat{x} \in \mathcal{X}_{\text{RoA}} = \{x \in \mathbb{R}^n \mid \hat{\Phi}(x)^\top P^{-1}\hat{\Phi}(x) \leq 1\}$ with probability $1 - \delta$.

Proof. As in Theorem 5, we divide the proof into two parts. We first show that all $x \in \mathcal{X}_{\text{RoA}}$ satisfy $(I_m \otimes \hat{\Phi}(x)) \in \mathbf{\Delta}$ and then conclude positive invariance of \mathcal{X}_{RoA} together with exponential stability of (1) for all $\hat{x} \in \mathcal{X}_{\text{RoA}}$.

Part I: $x \in \mathcal{X}_{\text{RoA}}$ implies $(I_m \otimes \hat{\Phi}(x)) \in \mathbf{\Delta}$: It can be shown analogously to the proof of Theorem 5 that all $x \in \mathcal{X}_{\text{RoA}}$ satisfy $\hat{\Phi}(x) \in \mathbf{\Delta}_\Phi$. More precisely, [43, Prop. 2] implies that $\Delta \in \mathbf{\Delta}$ if and only if $\Delta = I_m \otimes \Delta_\Phi$ with $\Delta_\Phi \in \mathbf{\Delta}_\Phi$. The claim then follows as $x \in \mathcal{X}_{\text{RoA}}$ implies $\hat{\Phi}(x) \in \mathbf{\Delta}_\Phi$.

Part II: Positive invariance of \mathcal{X}_{RoA} and exponential stability: For positive invariance of \mathcal{X}_{RoA} together with exponential stability of (1) for all $\hat{x} \in \mathcal{X}_{\text{RoA}}$, we define analogously to the proof of Theorem 5 the Lyapunov function candidate $V(x) = \hat{\Phi}(x)^\top P^{-1}\hat{\Phi}(x)$ such that positive invariance of \mathcal{X}_{RoA} can be deduced if $\frac{d}{dt}V(x(t)) \leq 0$ for all $x(t) \in \mathcal{X}_{\text{RoA}}$.

First, we define $K = LP^{-1}$ and $K_w = L_w(\Lambda^{-1} \otimes I_N)$, and denote $A_K = A + B_0K$ and $B_{K_w} = \tilde{B} + B_0K_w$. Then,

Algorithm 2 Flexible state-feedback controller design corresponding to Theorem 6.

Input:

- Data $\{x_j^{\bar{u}}, \dot{x}_j^{\bar{u}}\}_{j=1}^{d^{\bar{u}}}$ for $\bar{u} \in \{0, e_1, \dots, e_m\}$, where $d^{\bar{u}} \geq d_0$ for d_0 according to (20)
- Lifting $\Phi(x) = [1 \ \hat{\Phi}(x)]^\top$ defined in (6) satisfying Assumption 2
- Probabilistic tolerance $\delta \in (0, 1)$ and error bound $L_r > 0$
- Ellipsoidal region Δ_Φ defined by $Q_z \prec 0, S_z, R_z > 0$

Output: Exponentially stabilizing controller $u = \mu(x)$ for system (1) with probability $1 - \delta$ if $x \in \mathcal{X}_{\text{RoA}}$

Data-driven system representation:

Arrange the data according to (12) in $X^{\bar{u}}, Y^{\bar{u}}$

Solve the optimization problem (15) to obtain the data-based system matrices $A, B_0, \tilde{B} = [B_1 \ \dots \ B_m]$ according to Lemma 4

Controller design:

Solve the LMI feasibility problem in Theorem 6

if successful then

 Define the controller $\mu(x)$ as in (60)

end if

that the latter quantity Δ is, in fact, not unknown but can be used during operation to compute the feedback law. We note that Theorem 6 reduces to Theorem 5 for $m = 1$ and $L_w = 0$, i.e., a feedback that is linear in the lifted state. Due to its additional flexibility and more general controller structure, the design proposed in Theorem 6 allows for the consideration of larger error bounds L_r on the unknown remainder or is feasible even for potentially fewer data samples. Alternatively, the same amount of data can lead to a significantly increased region \mathcal{X}_{RoA} . Despite the more flexible controller structure, the controller design relies on the solution of an SDP in terms of LMI feasibility conditions and the resulting computational complexity remains comparable to the one of the feedback design in Section III. Hence, Theorem 6 establishes an efficiently solvable and flexible controller design with probabilistic guarantees for the *true* nonlinear system (1) based on sampled data, where the necessary amount of data d_0 is specified by (20) for a given desired probabilistic tolerance $\delta \in (0, 1)$ and a desired bound $L_r > 0$ on the remainder.

The overall controller design based on EDMD (15) and Theorem 6 is summarized in Algorithm 2.

V. ON THE GEOMETRY OF THE REGION OF ATTRACTION

In this section, we discuss specific properties of the guaranteed RoA resulting from its quadratic parametrization in lifted coordinates. Recall that our main results Theorem 5 and Theorem 6 guarantee exponential stability with a RoA given by a sublevel set of a quadratic Lyapunov function in the lifted space, i.e., $\mathcal{X}_{\text{RoA}} = \{x \in \mathbb{R}^n \mid \hat{\Phi}(x)^\top P^{-1} \hat{\Phi}(x) \leq 1\}$. In the following, we discuss that a suitable choice of P leading to a large RoA depends, as to be expected, on the distortion caused by the nonlinear lifting. In particular, we show that multiples of the identity matrix may not yield satisfactory results. These insights have direction implications for determining a suitable

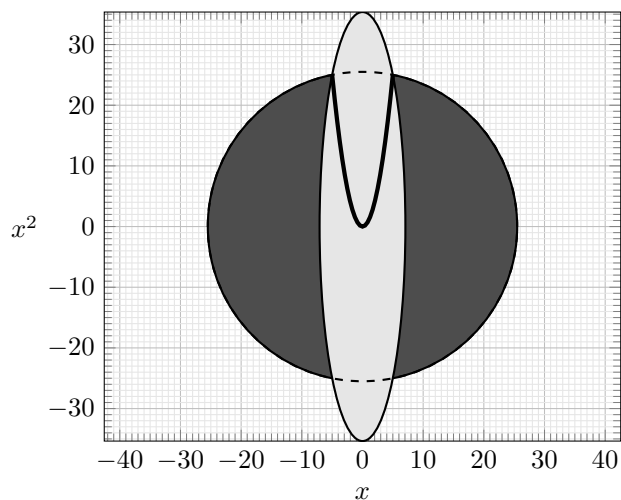


Fig. 1. Illustration of the regions Δ_x (—), $\Delta_{\Phi,1}$ (●), and $\Delta_{\Phi,2}$ (○).

choice of the matrices Q_z, S_z, R_z in (34), which parametrize the uncertainty description Δ_Φ characterizing the bilinear component of the dynamics.

As an instructive example, consider the lifting $\hat{\Phi}(x) = (x, x^2)$ with $x \in [-5, 5]$. Suppose we want to represent the set inclusion $x \in [-5, 5]$ via the set Δ_Φ , i.e., as a quadratic inequality in the lifted space. This can be done by defining Δ_Φ such that $\Delta_x = \{(x, x^2), x \in [-5, 5]\} \subseteq \Delta_\Phi$. The simple choice $Q_{z,1} = -I, S_{z,1} = 0, R_{z,1} = 650$ leads to

$$\Delta_{\Phi,1} = \{\Delta_\Phi \in \mathbb{R}^2 \mid \Delta_{\Phi,1}^2 + \Delta_{\Phi,2}^2 \leq 650\}, \quad (68)$$

corresponding to the parametrization of Δ_x as

$$\Delta_x = \{(x, x^2), x \in \mathbb{R} \mid x^2 + x^4 \leq 650\}. \quad (69)$$

This is, however, a non-ideal representation as it does not account for the fact that x^4 significantly outweighs x^2 when $|x| > 1$, and conversely for $|x| < 1$. Alternatively, we can, for example, rewrite

$$\Delta_x = \{(x, x^2), x \in \mathbb{R} \mid \frac{1}{2}(5^{-2}x^2 + 5^{-4}x^4) \leq 1\} \quad (70)$$

which leads with $Q_{z,2} = -\frac{1}{2} \text{diag}(5^{-2}, 5^{-4}), S_{z,2} = 0, R_{z,2} = 1$ to a more balanced parametrization

$$\Delta_{\Phi,2} = \{\Delta_\Phi \in \mathbb{R}^2 \mid \frac{1}{2}(5^{-2}\Delta_{\Phi,1}^2 + 5^{-4}\Delta_{\Phi,2}^2) \leq 1\}. \quad (71)$$

Although both $\Delta_{\Phi,1}$ and $\Delta_{\Phi,2}$ contain Δ_x , the volume of $\Delta_{\Phi,2}$ is significantly smaller than the volume of $\Delta_{\Phi,1}$, cf. Fig. 1. On the other hand, the nonlinear dependence of $\hat{\Phi}(x) = (x, x^2) \in \Delta_x$, i.e., the second entry is always the first entry squared, causes the same set Δ_x for both parametrizations (69) and (70). This nonlinear dependence is, however, neglected during controller design, where we over-approximate the bilinearity using the ellipsoidal descriptions $\Delta_{\Phi,1} \supseteq \Delta_x$ and $\Delta_{\Phi,2} \supseteq \Delta_x$ as shown in Fig. 1.

For the proposed controller design, the above observation is especially crucial because $Q_z, S_z,$ and R_z are fixed a-priori and they define an over-approximation of the RoA. In particular, the a-priori choice of Q_z determines the shape of the set Δ_Φ . Suitable choices of Q_z may allow for a larger RoA and should, thus, take the geometry of the RoA into account.

In the following, we propose a heuristic for determining a matrix Q_z based on the chosen lifting and the resulting EDMD-based estimated system matrices, i.e., A, B_0, B_1 or A, B_0, \tilde{B} corresponding to the steps for the data-driven system representation in Algorithm 1 or Algorithm 2, respectively.

Procedure 7. *The following steps lead to a non-trivial choice of Δ_Φ which takes the structure of the lifting into account:*

- 1) Define $Q_z = -I$, $S_z = 0$, and $R_z > 0$.
- 2) Find
 - a) for Algorithm 1: $\hat{P} = \hat{P}^\top \succ 0$, $\hat{L}, \hat{\lambda} > 0$, $\hat{\tau} > 0$ such that (38), or
 - b) for Algorithm 2: $\hat{P} = \hat{P}^\top \succ 0$, $\hat{L}, \hat{L}_w, \hat{\Lambda} = \hat{\Lambda}^\top \succ 0$, $\hat{\tau} > 0$ such that (58).
- 3) Define Δ_Φ via $Q_z = -\frac{\hat{P}^{-1}}{\|\hat{P}^{-1}\|_2}$, $S_z = 0$, and $R_z > 0$.

After defining Δ_Φ , we can proceed as stated in the controller design of Algorithm 1 or Algorithm 2. The steps in Procedure 7 solve the proposed controller design once without enforcing the RoA to be robust positively invariant. This results in the SDP-optimization having more degrees of freedom to find a suitable shape of the ellipsoidal RoA defined by \hat{P} . As a consequence, the optimization can find a shape that naturally takes the dynamics *and* the structure of the lifting function into account. Further, it allows to define the uncertainty region Δ_Φ such that the shape of the obtained RoA \mathcal{X}_{RoA} of the controller design is more similar to the shape of Δ_Φ itself and, thus, reduces conservatism in the robust controller design. A rigorous investigation of the resulting RoA for a specific choice of Δ_Φ is a promising path for future work.

VI. NUMERICAL EXAMPLES

In the following, we illustrate the proposed controller design in numerical examples. We conduct the simulations in Matlab using the toolbox YALMIP [64] with the SDP solver MOSEK [65].

A. Nonlinear system with invariant Koopman lifting

Consider the nonlinear system (cf. [35])

$$\dot{x}_1(t) = \mu x_1(t), \quad (72a)$$

$$\dot{x}_2(t) = \lambda(x_2(t) - x_1(t)^2) + u(t). \quad (72b)$$

with $\mu, \lambda \in \mathbb{R}$. To obtain a Koopman-based surrogate model, we define the lifting function $\hat{\Phi}$ as

$$\hat{\Phi}(x) = \left[x_1 \quad x_2 \quad x_2 - \frac{\lambda}{\lambda - 2\mu} x_1^2 \right]^\top. \quad (73)$$

A particular feature of (72) is that we can derive an exact finite-dimensional lifted bilinear representation given by

$$\begin{aligned} \frac{d}{dt} \hat{\Phi}(x(t)) &= \left(\nabla \hat{\Phi}(x(t)) \right)^\top \left(\frac{d}{dt} x(t) \right) \\ &= \begin{bmatrix} \mu x_1(t) \\ \lambda(x_2(t) - x_1(t)^2) + u(t) \\ -\frac{2\lambda\mu}{\lambda - 2\mu} x_1(t)^2 + \lambda(x_2(t) - x_1(t)^2) + u(t) \end{bmatrix} \\ &= \begin{bmatrix} \mu & 0 & 0 \\ 0 & 2\mu & \lambda - 2\mu \\ 0 & 0 & \lambda \end{bmatrix} \hat{\Phi}(x(t)) + \begin{bmatrix} 0 \\ 1 \\ 1 \end{bmatrix} u(t). \end{aligned}$$

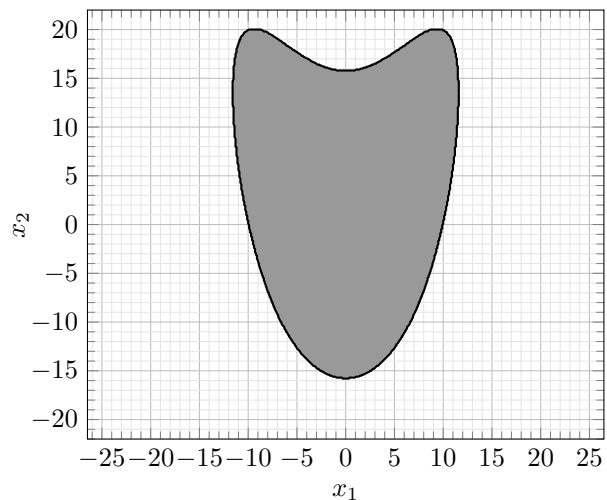


Fig. 2. RoA \mathcal{X}_{RoA} corresponding to Section VI-A and the controller μ .

In the following, we choose $\mu = -2$ and $\lambda = 1$. Since we assume that the system dynamics are unknown but we have only access to data samples, we use EDMD for a data-driven approximation. For a data length of $d = 5000$, where the data samples are uniformly sampled from the sets $\mathbb{X} = [-1, 1]^2$ and $\mathbb{U} = [-1, 1]$, the EDMD optimization (15) yields the data-based lifted system dynamics (31) with

$$A = \begin{bmatrix} -2.0 & 0 & 0 \\ 0 & -4.0 & 5.0 \\ 0 & 0 & 1.0 \end{bmatrix}, B_0 = \begin{bmatrix} 0 \\ 1.0 \\ 1.0 \end{bmatrix}, B_1 = \begin{bmatrix} 0 & 0 & 0 \\ 0 & 0 & 0 \\ 0 & 0 & 0 \end{bmatrix}.$$

To account for a possible sampling error, we choose $L_r = 0.1$ and the probabilistic tolerance $\delta = 0.05$, cf. Proposition 3. Here, the choice of $d = 5000$ results in the approximators A, B_0, B_1 being accurate up to 13 digits.

To apply the proposed controller design, we define the ellipsoidal region Δ_Φ via $Q_z = -I$, $S_z = 0$, and $R_z = 500$. Following Algorithm 1 for the simplified controller design, we obtain the state-feedback control law

$$\mu(x) = [0.00 \quad -3.77 \quad -3.46] \hat{\Phi}(x).$$

Here, Algorithm 2 for the more flexible state-feedback controller yields $L_w = 0$ and, hence, the same controller μ . This can be explained by the linear structure of the lifted dynamics, allowing to achieve satisfactory control performance already with a linear state feedback. The above controller stabilizes the closed loop of (72) in the RoA depicted in Fig. 2. We note that the resulting RoA for this example is such that $\hat{\Phi}(x) \in \Delta$ if and only if $x \in \mathcal{X}_{\text{RoA}}$, i.e., the region Δ_Φ characterizing the artificially introduced uncertainty only contains x which are contained in the RoA as well. Hence, the designed controller, which is robust w.r.t. to all $\Delta_\Phi \in \Delta_\Phi$, is only robust w.r.t. $x \in \text{RoA}$ and adds no conservatism by accounting also for some $x \notin \mathcal{X}_{\text{RoA}}$.

Remark 8. *For the considered system (72) and lifting $\hat{\Phi}$, Lemma 4 guarantees the upper bound (26) on the remainder if $d \geq d_0$, where d_0 characterizes the sufficient number of data points defined in (20). This bound can be evaluated if*

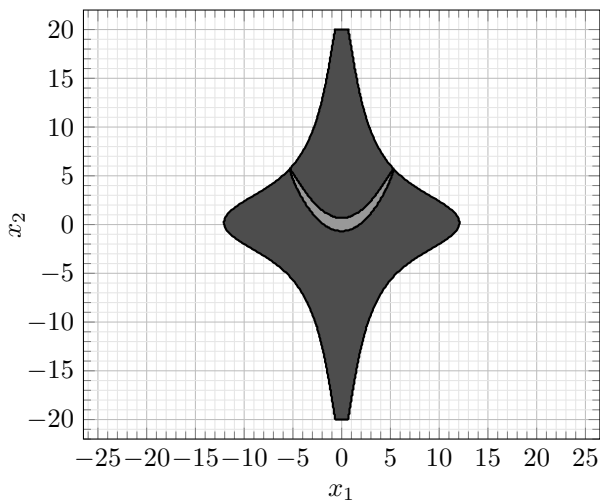


Fig. 3. Region containing all x with $\hat{\Phi}(x) \in \Delta_\Phi$ (●) corresponding to Section VI-B and the RoA \mathcal{X}_{RoA} (○) for the controller μ_1 .

the system dynamics are known. In particular, the bound yields $d_0 = 6.9 \times 10^{17}$ for this example. We emphasize that this bound is clearly conservative and, as demonstrated above, already less data leads to an accurate data-driven approximation of the true system. The conservatism is expected to be due to the validity of the bound for general system classes.

B. Nonlinear system without invariant Koopman lifting

The example in Section VI-A is based on a lifting function that results in a perfect (bi-)linear representation of the dynamics. Since this is rarely the case in practice, we include an additional lifting function in the following. As before, we consider the nonlinear system (72) with $\mu = -2$ and $\lambda = 1$, but additionally include the lifting function $\phi_4(x) = x_1 x_2$ resulting in the lifting function

$$\hat{\Phi}(x) = \left[x_1 \quad x_2 \quad x_2 - \frac{\lambda}{\lambda - 2\mu} x_1^2 \quad x_1 x_2 \right]^\top.$$

Note that the corresponding dictionary is not invariant under the system dynamics (72) and thereby violates Assumption 2. In the following, however, we show that the proposed approach still produces reliable results. For the data generation, we sample again $d = 5000$ data points uniformly from the interval $\mathbb{X} = [-1, 1]^2$ and $\mathbb{U} = [-1, 1]$ yielding a lifted bilinear representation (31), where we assume that the remainder is bounded by (26) with $L_r = 0.01$ and probabilistic tolerance $\delta = 0.05$. Further, we implement Algorithm 2 for the ellipsoidal region Δ_Φ based on $Q_z = -I$, $S_z = 0$, and $R_z = 1000$ leading to the controller

$$\mu_1(x) = \frac{\begin{bmatrix} -0.0001 & -0.0132 & -2.8888 & 0.0001 \end{bmatrix} \hat{\Phi}(x)}{1 - \begin{bmatrix} 0.0001 & -0.0000 & -0.0000 & -0.0000 \end{bmatrix} \hat{\Phi}(x)}$$

stabilizing the closed-loop of (72) in the RoA depicted in Fig. 3. Recall that the region Δ_Φ is chosen and fixed prior to the controller design. The controller design then optimizes for a controller guaranteeing closed-loop stability for a large RoA. Ideally, this RoA contains all x with $\hat{\Phi}(x) \in \Delta_\Phi$ and, hence, a good a-priori choice of Δ_Φ is critical (cf. Section V). Whereas

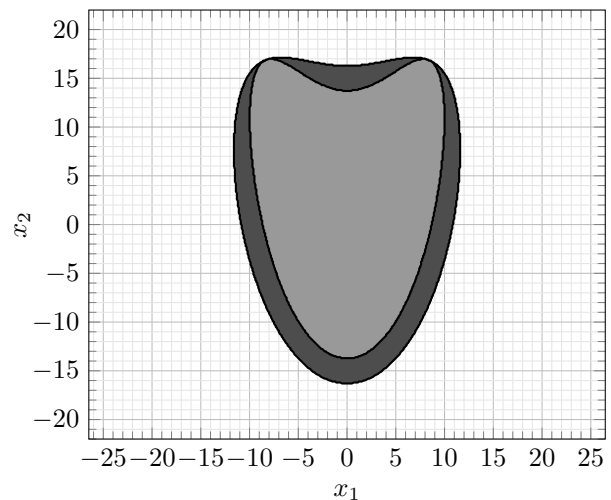


Fig. 4. Region containing all x with $\hat{\Phi}(x) \in \Delta_\Phi$ (●) corresponding to Section VI-B and the RoA \mathcal{X}_{RoA} (○) for the controller μ_2 .

this was indeed achieved by the controller in Section VI-A, the resulting RoA in Fig. 3 contains only a small portion of all $x \in \mathbb{R}^2$ satisfying $\hat{\Phi} \in \Delta_\Phi$. This is a clear indication that the chosen Δ_Φ is not optimal w.r.t. the used lifting functions and the underlying nonlinear dynamics (72).

To investigate this further, we consider the same setting as before but with a different choice of Δ_Φ . In particular, we define Δ_Φ again via $S_z = 0$ and $R_z = 1000$, but with the more sophisticated choice of $Q_z = -\text{diag}(2.5, 2.5, 1.25, 0.005)$ with an individual weight for each lifting function. Then, Algorithm 2 yields the controller

$$\mu_2(x) = \frac{\begin{bmatrix} -0.0049 & -2.0567 & -2.4020 & -0.0092 \end{bmatrix} \hat{\Phi}(x)}{1 - \begin{bmatrix} 0.0053 & -0.0000 & -0.0000 & -0.0001 \end{bmatrix} \hat{\Phi}(x)}$$

stabilizing the closed-loop of (72) in the RoA depicted in Fig. 4. We stress that this RoA a) is significantly larger and b) provides a more accurate cover of the region of all x with $\hat{\Phi}(x) \in \Delta_\Phi$ than the one for Δ_Φ based on $Q_z = -I$. This illustrates the important role of the shape of Δ_Φ in the proposed controller design.

C. Inverted pendulum

To illustrate our controller design with an actually physical example, we investigate an inverted pendulum which is a well-used benchmark for nonlinear controller design methods (cf. [1], [13], [15], [66], [67] and references therein). To this end, we consider the dynamics

$$\dot{x}_1(t) = x_2(t), \quad (74a)$$

$$\dot{x}_2(t) = \frac{g}{l} \sin(x_1(t)) - \frac{b}{ml^2} x_2(t) + \frac{1}{ml^2} u(t) \quad (74b)$$

with mass m , length l , rotational friction coefficient b , and gravitational constant $g = 9.81$ m/s. For the simulation, we choose $m = 1$, $l = 1$, and $b = 0.01$. We define the lifting function $\hat{\Phi}(x) = [x_1 \quad x_2 \quad \sin(x_1)]^\top$ and use $d = 15000$ data points uniformly sampled from $\mathbb{X} = [-2, 10]^2$ and

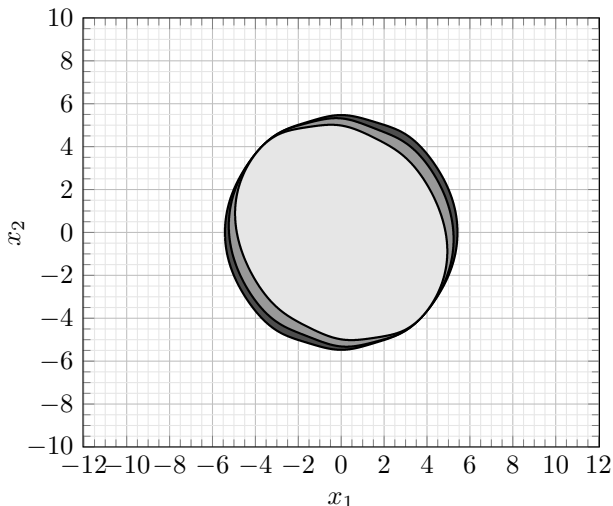


Fig. 5. Region containing all x with $\hat{\Phi}(x) \in \Delta_{\Phi}$ (●) corresponding to Section VI-C, the RoA \mathcal{X}_{RoA} (○) for the controller μ_1 , and the RoA \mathcal{X}_{RoA} (○) for the controller μ_2 .

$\mathbb{U} = [-10, 10]$. This leads to the data-driven bilinear Koopman surrogate model (31) with

$$A = \begin{bmatrix} 0 & 1.00 & 0 \\ 0 & -0.50 & 9.81 \\ -0.17 & 0.13 & 0.03 \end{bmatrix},$$

$$B_0 = \begin{bmatrix} 0 \\ 1.00 \\ 1.12 \end{bmatrix}, \quad B_1 = \begin{bmatrix} 0 & 0 & 0 \\ 0 & 0 & 0 \\ -0.10 & -0.10 & 0.13 \end{bmatrix},$$

where the remainder $\hat{r}(x, u)$ is bounded by (26) with $L_r = 0.02$ and probabilistic tolerance $\delta = 0.05$. In the following, we compare two different choices for the region Δ_{Φ} and their implications for the application of Algorithms 1 and 2.

1) First, we use the straightforward definition of Δ_{Φ} via $Q_z = -I$, $S_z = 0$, and $R_z = 30$. Then, Algorithm 1 and Algorithm 2 yield the simplified state feedback

$$\mu_1(x) = [-1.4095 \quad -8.1208 \quad -8.8105] \hat{\Phi}(x)$$

and the more flexible state feedback

$$\mu_2(x) = \frac{[-0.5967 \quad -6.5454 \quad -4.6422] \hat{\Phi}(x)}{1 - [0.0453 \quad 0.0435 \quad -0.0579] \hat{\Phi}(x)}$$

with the respective RoA depicted in Fig. 5. While the resulting RoAs acceptably cover the region corresponding to Δ_{Φ} , the RoA for both μ_1 and μ_2 are ellipsoidal. This indicates that the ellipsoidal region Δ_{Φ} for $\hat{\Phi}(x)$ constrains mostly the state x itself. Hence, the presented robust controller design has to account for a possibly unnecessarily large uncertainty region.

2) As a remedy, we define Δ_{Φ} now based on the proposed heuristic in Section V. In particular, we first follow the steps of Procedure 7 to obtain a non-trivial choice of Q_z . This matrix is then used to define the shape of Δ_{Φ} . As before, we choose $S_z = 0$ and use $R_z = 5$ to scale the overall size of the region. Applying Algorithms 1 and 2 yields the controllers

$$\mu_3(x) = [-3.2179 \quad -2.8083 \quad -13.6730] \hat{\Phi}(x) \quad (75)$$

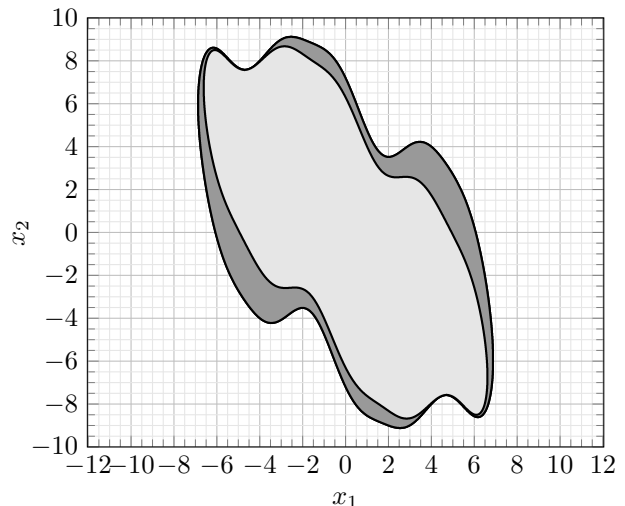


Fig. 6. Region containing all x with $\hat{\Phi}(x) \in \Delta_{\Phi}$ (●) corresponding to Section VI-C, the RoA \mathcal{X}_{RoA} (○) for the controller μ_3 , and the RoA \mathcal{X}_{RoA} (○) for the controller μ_4 .

and

$$\mu_4(x) = \frac{[-1.6091 \quad -1.3541 \quad -8.3180] \hat{\Phi}(x)}{1 - [0.0493 \quad 0.0469 \quad -0.0610] \hat{\Phi}(x)} \quad (76)$$

stabilizing the closed-loop of (74) in the significantly larger RoA depicted in Fig. 6.

VII. CONCLUSION

In this paper, we presented a robust controller design to overcome challenges posed by finite-dimensional and data-driven approximations of Koopman surrogate models. In particular, we designed a flexible state-feedback controller based on the lifted system dynamics ensuring end-to-end stability guarantees for the true nonlinear system. Moreover, our method established a crucial connection between closed-loop guarantees and the required data for a probabilistic bound on the approximation error. Further, we used semidefinite programming and linear matrix inequalities to ensure an efficient and reliable design procedure. The tutorial-style explanation of our results in Section III enhanced accessibility and our extension to more flexible nonlinear state-feedback controllers in Section IV reduced the conservatism of the approach. The broad applicability of the presented controller design framework was illustrated in numerical examples.

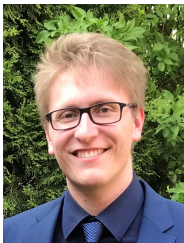
In future work, we aim to explicitly address the projection error due to an approximate and finite set of dictionary functions, considering a potential transition to a reproducing Kernel Hilbert space setting [34]. Additionally, we plan to explore alternative sampling strategies beyond the currently employed uniform sampling strategy. This includes investigating the use of trajectory data for specific inputs and exploring derivative-free data acquisition methods.

REFERENCES

- [1] T. Martin, T. B. Schön, and F. Allgöwer, “Guarantees for data-driven control of nonlinear systems using semidefinite programming: A survey,” *Annual Reviews in Control*, p. 100911, 2023.

- [2] J. C. Willems, P. Rapisarda, I. Markovskiy, and B. L. De Moor, "A note on persistency of excitation," *Systems & Control Letters*, vol. 54, no. 4, pp. 325–329, 2005.
- [3] C. De Persis and P. Tesi, "Formulas for data-driven control: Stabilization, optimality, and robustness," *IEEE Transactions on Automatic Control*, vol. 65, no. 3, pp. 909–924, 2019.
- [4] J. Berberich, A. Koch, C. W. Scherer, and F. Allgöwer, "Robust data-driven state-feedback design," in *Proc. IEEE American Control Conference (ACC)*, 2020, pp. 1532–1538.
- [5] H. J. van Waarde, J. Eising, H. L. Trentelman, and M. K. Camlibel, "Data informativity: a new perspective on data-driven analysis and control," *IEEE Transactions on Automatic Control*, vol. 65, no. 11, pp. 4753–4768, 2020.
- [6] Z.-S. Hou and Z. Wang, "From model-based control to data-driven control: Survey, classification and perspective," *Information Sciences*, vol. 235, pp. 3–35, 2013.
- [7] I. Markovskiy and F. Dörfler, "Behavioral systems theory in data-driven analysis, signal processing, and control," *Annual Reviews in Control*, vol. 52, pp. 42–64, 2021.
- [8] T. Faulwasser, R. Ou, G. Pan, P. Schmitz, and K. Worthmann, "Behavioral theory for stochastic systems? A data-driven journey from Willems to Wiener and back again," *Annual Reviews in Control*, vol. 55, pp. 92–117, 2023.
- [9] J. Berberich and F. Allgöwer, "A trajectory-based framework for data-driven system analysis and control," in *Proc. IEEE European Control Conference (ECC)*, 2020, pp. 1365–1370.
- [10] A. Bisoffi, C. De Persis, and P. Tesi, "Data-based stabilization of unknown bilinear systems with guaranteed basin of attraction," *Systems & Control Letters*, vol. 145, p. 104788, 2020.
- [11] M. Guo, C. De Persis, and P. Tesi, "Data-driven stabilization of nonlinear polynomial systems with noisy data," *IEEE Transactions on Automatic Control*, vol. 67, no. 8, pp. 4210–4217, 2022.
- [12] T. Dai and M. Sznaier, "A semi-algebraic optimization approach to data-driven control of continuous-time nonlinear systems," *IEEE Control Systems Letters*, vol. 5, no. 2, pp. 487–492, 2021.
- [13] R. Strässer, J. Berberich, and F. Allgöwer, "Data-driven control of nonlinear systems: Beyond polynomial dynamics," in *Proc. 60th IEEE Conference on Decision and Control (CDC)*, 2021, pp. 4344–4351.
- [14] T. Martin and F. Allgöwer, "Data-driven system analysis of nonlinear systems using polynomial approximation," *IEEE Transactions on Automatic Control*, 2023.
- [15] T. Martin, T. B. Schön, and F. Allgöwer, "Gaussian inference for data-driven state-feedback design of nonlinear systems," *IFAC-PapersOnLine*, vol. 56, no. 2, pp. 4796–4803, 2023, 22nd IFAC World Congress.
- [16] C. Fiedler, C. W. Scherer, and S. Trimpe, "Learning-enhanced robust controller synthesis with rigorous statistical and control-theoretic guarantees," in *Proc. 60th IEEE Conference on Decision and Control (CDC)*, 2021, pp. 5122–5129.
- [17] A. Devonport, H. Yin, and M. Arcak, "Bayesian safe learning and control with sum-of-squares analysis and polynomial kernels," in *Proc. 59th IEEE Conference on Decision and Control (CDC)*, 2020, pp. 3159–3165.
- [18] C. Verhoek, P. J. Koelewijn, S. Haesaert, and R. Tóth, "Direct data-driven state-feedback control of general nonlinear systems," *arXiv:2303.10648*, 2023.
- [19] J. Miller and M. Sznaier, "Data-driven gain scheduling control of linear parameter-varying systems using quadratic matrix inequalities," *IEEE Control Systems Letters*, vol. 7, pp. 835–840, 2023.
- [20] B. O. Koopman, "Hamiltonian systems and transformation in Hilbert space," *Proc. of the National Academy of Sciences of the United States of America*, vol. 17, no. 5, p. 315, 1931.
- [21] I. Mezić, "Spectral properties of dynamical systems, model reduction and decompositions," *Nonlinear Dynamics*, vol. 41, no. 1-3, pp. 309–325, 2005.
- [22] J. L. Proctor, S. L. Brunton, and J. N. Kutz, "Generalizing Koopman theory to allow for inputs and control," *SIAM Journal on Applied Dynamical Systems*, vol. 17, no. 1, pp. 909–930, 2018.
- [23] S. E. Otto and C. W. Rowley, "Koopman operators for estimation and control of dynamical systems," *Annual Review of Control, Robotics, and Autonomous Systems*, vol. 4, pp. 59–87, 2021.
- [24] A. Mauroy, I. Mezić, and Y. Susuki, *The Koopman operator in systems and control*. Springer, 2020.
- [25] P. Bevanda, S. Sosnowski, and S. Hirche, "Koopman operator dynamical models: Learning, analysis and control," *Annual Reviews in Control*, vol. 52, pp. 197–212, 2021.
- [26] M. Williams, I. Kevrekidis, and C. Rowley, "A data-driven approximation of the Koopman operator: Extending dynamic mode decomposition," *Journal of Nonlinear Science*, vol. 25, no. 6, pp. 1307–1346, 08 2015.
- [27] M. Korda and I. Mezić, "On convergence of extended dynamic mode decomposition to the Koopman operator," *Journal of Nonlinear Science*, vol. 28, no. 2, pp. 687–710, 2018.
- [28] M. Haseli and J. Cortés, "Temporal forward-backward consistency, not residual error, measures the prediction accuracy of extended dynamic mode decomposition," *IEEE Control Systems Letters*, vol. 7, pp. 649–654, 2023.
- [29] N. Takeishi, Y. Kawahara, and T. Yairi, "Learning Koopman invariant subspaces for dynamic mode decomposition," *Advances in neural information processing systems*, vol. 30, 2017.
- [30] S. E. Otto and C. W. Rowley, "Linearly recurrent autoencoder networks for learning dynamics," *SIAM Journal on Applied Dynamical Systems*, vol. 18, no. 1, pp. 558–593, 2019.
- [31] Y. Chen and U. Vaidya, "Sample complexity for nonlinear stochastic dynamics," in *Proc. IEEE American Control Conference (ACC)*, 2019, pp. 3526–3531.
- [32] F. Nüske, S. Peitz, F. Philipp, M. Schaller, and K. Worthmann, "Finite-data error bounds for Koopman-based prediction and control," *Journal of Nonlinear Science*, vol. 33, no. 1, p. 14, 2023.
- [33] M. Schaller, K. Worthmann, F. Philipp, S. Peitz, and F. Nüske, "Towards reliable data-based optimal and predictive control using extended DMD," *IFAC-PapersOnLine*, vol. 56, no. 1, pp. 169–174, 2023.
- [34] F. Philipp, M. Schaller, K. Worthmann, S. Peitz, and F. Nüske, "Error bounds for kernel-based approximations of the Koopman operator," *arXiv:2301.08637*, 2023.
- [35] S. L. Brunton, B. W. Brunton, J. L. Proctor, and J. N. Kutz, "Koopman invariant subspaces and finite linear representations of nonlinear dynamical systems for control," *PloS one*, vol. 11, no. 2, pp. 1–19, 2016.
- [36] M. Korda and I. Mezić, "Linear predictors for nonlinear dynamical systems: Koopman operator meets model predictive control," *Automatica*, vol. 93, pp. 149–160, 2018.
- [37] S. Sinha, S. P. Nandanoori, J. Drgona, and D. Vrabie, "Data-driven stabilization of discrete-time control-affine nonlinear systems: A Koopman operator approach," in *Proc. IEEE European Control Conference (ECC)*, 2022, pp. 552–559.
- [38] D. Bruder, X. Fu, R. B. Gillespie, C. D. Remy, and R. Vasudevan, "Koopman-based control of a soft continuum manipulator under variable loading conditions," *IEEE Robotics and Automation Letters*, vol. 6, no. 4, pp. 6852–6859, 2021.
- [39] J. S. Kim, Y. S. Quan, and C. C. Chung, "Koopman operator-based model identification and control for automated driving vehicle," *International Journal of Control, Automation and Systems*, vol. 21, no. 8, pp. 2431–2443, 2023.
- [40] M. Budišić, R. Mohr, and I. Mezić, "Applied Koopmanism," *Chaos: An Interdisciplinary Journal of Nonlinear Science*, vol. 22, no. 4, 2012.
- [41] R. Strässer, J. Berberich, and F. Allgöwer, "Robust data-driven control for nonlinear systems using the Koopman operator*," *IFAC-PapersOnLine*, vol. 56, no. 2, pp. 2257–2262, 2023, 22nd IFAC World Congress.
- [42] L. Bold, L. Grüne, M. Schaller, and K. Worthmann, "Practical asymptotic stability of data-driven model predictive control using extended DMD," *arXiv:2308.00296*, 2023.
- [43] R. Strässer, J. Berberich, and F. Allgöwer, "Control of bilinear systems using gain-scheduling: Stability and performance guarantees," *Proc. 62nd IEEE Conference on Decision and Control (CDC) (to appear)*, Preprint: *arXiv:2304.04486*, 2023.
- [44] M. Eyüboğlu, N. R. Powell, and A. Karimi, "Data-driven control synthesis using Koopman operator: A robust approach," 2024.
- [45] P. van Goor, R. Mahony, M. Schaller, and K. Worthmann, "Reprojection methods for Koopman-based modelling and prediction," *Proc. 62nd IEEE Conference on Decision and Control (CDC) (to appear)*, Preprint: *arXiv:2307.16188*, 2023.
- [46] M. O. Williams, M. S. Hemati, S. T. Dawson, I. G. Kevrekidis, and C. W. Rowley, "Extending data-driven Koopman analysis to actuated systems," *IFAC-PapersOnLine*, vol. 49, no. 18, pp. 704–709, 2016.
- [47] A. Surana, "Koopman operator based observer synthesis for control-affine nonlinear systems," in *Proc. 55th IEEE Conf. Decision Control (CDC)*, 2016, pp. 6492–6499.
- [48] S. Peitz, S. E. Otto, and C. W. Rowley, "Data-driven model predictive control using interpolated Koopman generators," *SIAM J. Applied Dynamical Systems*, vol. 19, no. 3, pp. 2162–2193, 2020.

- [49] S. Klus, F. Nüske, S. Peitz, J.-H. Niemann, C. Clementi, and C. Schütte, “Data-driven approximation of the Koopman generator: Model reduction, system identification, and control,” *Physica D: Nonlinear Phenomena*, vol. 406, p. 132416, 2020.
- [50] C. Zhang and E. Zuazua, “A quantitative analysis of Koopman operator methods for system identification and predictions,” *Comptes Rendus. Mécanique*, vol. 351, no. S1, pp. 1–31, 2023.
- [51] S. Klus, F. Nüske, and B. Hamzi, “Kernel-based approximation of the Koopman generator and Schrödinger operator,” *Entropy*, vol. 22, no. 7, p. 722, 2020.
- [52] M. O. Williams, C. W. Rowley, and I. G. Kevrekidis, “A kernel-based method for data-driven Koopman spectral analysis,” *Journal of Computational Dynamics*, vol. 2, no. 2, pp. 247–265, 2016.
- [53] D. Goswami and D. A. Paley, “Bilinearization, reachability, and optimal control of control-affine nonlinear systems: A Koopman spectral approach,” *IEEE Transactions on Automatic Control*, vol. 67, no. 6, pp. 2715–2728, 2021.
- [54] M. Korda and I. Mezić, “Optimal construction of Koopman eigenfunctions for prediction and control,” *IEEE Transactions on Automatic Control*, vol. 65, no. 12, pp. 5114–5129, 2020.
- [55] L. C. Iacob, R. Tóth, and M. Schoukens, “Koopman form of nonlinear systems with inputs,” *arXiv:2207.12132*, 2022.
- [56] M. Haseli and J. Cortés, “Invariance proximity: Closed-form error bounds for finite-dimensional Koopman-based models,” *arXiv:2311.13033*, 2023.
- [57] K. Zhou, J. C. Doyle, K. Glover *et al.*, *Robust and optimal control*. Prentice Hall New Jersey, 1996, vol. 40.
- [58] S. P. Boyd and L. Vandenberghe, *Convex Optimization*. Cambridge University Press, 2004.
- [59] C. W. Scherer and S. Weiland, “Linear matrix inequalities in control,” *Lecture Notes, Dutch Institute for Systems and Control, Delft, The Netherlands*, vol. 3, no. 2, 2000.
- [60] C. W. Scherer, “LPV control and full block multipliers,” *Automatica*, vol. 37, no. 3, pp. 361–375, 2001.
- [61] J. C. Doyle, K. Glover, P. P. Khargonekar, and B. A. Francis, “State-space solutions to standard H_2 and H_∞ control problems,” *IEEE Transactions on Automatic Control*, vol. 34, no. 8, pp. 831–847, 1989.
- [62] A. Packard, K. Zhou, P. Pandey, J. Leonhardson, and G. Balas, “Optimal, constant I/O similarity scaling for full-information and state-feedback control problems,” *Systems & Control Letters*, vol. 19, no. 4, pp. 271–280, 1992.
- [63] A. Astolfi, “On the relation between state feedback and full information regulators in nonlinear singular H_∞ control,” *IEEE Transactions on Automatic Control*, vol. 42, no. 7, pp. 984–988, 1997.
- [64] J. Löfberg, “YALMIP: A toolbox for modeling and optimization in MATLAB,” in *Proc. IEEE International Conference on Robotics and Automation*, 2004, pp. 284–289.
- [65] M. ApS, *The MOSEK optimization toolbox for MATLAB manual. Version 9.3.21*, 2022.
- [66] M. Tiwari, G. Nehma, and B. Lusch, “Computationally efficient data-driven discovery and linear representation of nonlinear systems for control,” *arXiv:2309.04074*, 2023.
- [67] C. Verhoek, H. S. Abbas, and R. Tóth, “Direct data-driven LPV control of nonlinear systems: An experimental result,” *arXiv:2211.17191*, 2022.



Data-Integrated Simulation Science (SimTech2023).

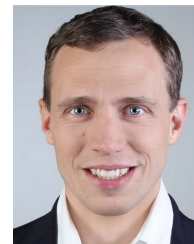
Robin Strässer (Graduate Student Member, IEEE) received a master’s degree in Simulation Technology from the University of Stuttgart, Stuttgart, Germany, in 2020. Since 2020, he has been a Research and Teaching Assistant with the Institute for Systems Theory and Automatic Control and a member of the Graduate School Simulation Technology, University of Stuttgart. His research interests include data-driven system analysis and control with focus on nonlinear systems. Robin Strässer received the Best Poster Award at the International Conference on



fellow of the GAMM (Society for Applied Mathematics and Mechanics) and received the Best Poster Award at the workshop on systems theory and PDEs (WOSTAP 2022).

Manuel Schaller obtained the M.Sc. and Ph.D. in Applied Mathematics from the University of Bayreuth in 2017 and 2021 respectively. From 2020–2023 he held a PostDoc and Lecturer (tenure track) position in the Optimization-based Control group at Technische Universität Ilmenau, Germany. There, he is Assistant Professor for differential equations since July 2023. His research focuses on data-driven control with guarantees, port-Hamiltonian systems and stability in infinite dimensional optimal control.

For his research Dr. Schaller has been named junior



appointed Junior Fellow of the Society of Applied Mathematics and Mechanics (GAMM), where he served as speaker in 2014 and 2015. His current research interests include systems and control theory with a particular focus on nonlinear model predictive control, stability analysis, and data-driven control.

Karl Worthmann received his Ph.D. degree in mathematics from the University of Bayreuth, Germany, in 2012. 2014 he became assistant professor for “Differential Equations” at Technische Universität Ilmenau (TU Ilmenau), Germany. 2019 he was promoted to full professor after receiving the Heisenberg-professorship “Optimization-based Control” by the German Research Foundation (DFG). He was recipient of the Ph.D. Award from the City of Bayreuth, Germany, and stipend of the German National Academic Foundation. 2013 he has been



Control in 2020 and the 2022 George S. Axelby Outstanding Paper Award. His research interests include data-driven analysis and control as well as quantum computing.

Julian Berberich received an M.Sc. degree in Engineering Cybernetics from the University of Stuttgart, Germany, in 2018. In 2022, he obtained a Ph.D. in Mechanical Engineering, also from the University of Stuttgart, Germany. He is currently working as a Lecturer (Akademischer Rat) at the Institute for Systems Theory and Automatic Control at the University of Stuttgart, Germany. In 2022, he was a visiting researcher at the ETH Zürich, Switzerland. He has received the Outstanding Student Paper Award at the 59th IEEE Conference on Decision and



with application to a wide range of fields including systems biology. Dr. Allgöwer was the President of the International Federation of Automatic Control (IFAC) in 2017–2020 and the Vice President of the German Research Foundation DFG in 2012–2020.

Frank Allgöwer (Member, IEEE) studied engineering cybernetics and applied mathematics in Stuttgart and with the University of California, Los Angeles (UCLA), CA, USA, respectively, and received the Ph.D. degree from the University of Stuttgart, Stuttgart, Germany. Since 1999, he has been the Director of the Institute for Systems Theory and Automatic Control and a professor with the University of Stuttgart. His research interests include predictive control, data-based control, networked control, cooperative control, and nonlinear control